Monitoring and simulation of ground deformations by super-large EPB culvert jacking tunnelling combining with pipe-roof preconstruction method (PPM) in urban environments

Zhang, Xuehui; Qin, Jiantuan; Zhang, Xiao; Zhang, Jiarui; Jiang, Xi

DOI
10.1016/j.tust.2025.106909

Publication date
2025

Document Version
Final published version

Published in
Tunnelling and Underground Space Technology

Tunnelling and Underground Space Technology 165 (2025) 106909

Contents lists available at ScienceDirect

Tunnelling and Underground Space Technology incorporating Trenchless Technology Research

journal homepage: www.elsevier.com/locate/tust

Monitoring and simulation of ground deformations by super-large EPB culvert jacking tunnelling combining with pipe-roof preconstruction method (PPM) in urban environments☆

Xuehui Zhang [a], Jiantuan Qin [b], Xiao Zhang [c], Jiarui Zhang [d,*], Xi Jiang [e]

[a] Department of Civil and Environmental Engineering, The Hong Kong Polytechnic University, Hung Hom, Kowloon, Hong Kong Special Administrative Region
[b] School of Construction Engineering, Guangxi Vocational and Technical Institute of Industry, Nanning, Guangxi, China
[c] Shanghai Urban Construction Municipal Engineering (Group) Co. Ltd., Shanghai 200065, China
[d] Geo-Engineering Section, Department of Geo-science and Engineering, Delft University of Technology, Delft, The Netherlands
[e] Department of Geotechnical Engineering, Tongji University, Shanghai, China

ARTICLE INFO

Keywords:
Culvert Jacking Tunnelling
Pipe-roof Preconstruction Method (PPM)
Ground Settlement
Urban tunnelling
Shallow Tunnelling

ABSTRACT

Earth pressure balance (EPB) culvert jacking tunnelling, combining with pipe-roof preconstruction method (PPM), offers a competent solution particularly for constructing large shallow underpass tunnels in urban environments. However, technical knowledge gaps exist regarding its applicability, primarily due to a lack of project case studies and field monitoring data. This study specifically investigates the ground deformation characteristics associated with EPB culvert jacking tunnelling, based on the world's largest to date culvert-jacked tunnel (19.8 m wide and 6.4 m high) project utilizing PPM in soft ground in China. The study provides a detailed analysis of the deformation time-history of both the ground surface and the pipe roof. Additionally, a three-dimensional numerical simulation is conducted to explore the correlation between ground deformation and both front face and lubrication grouting pressures. The key findings include that: (1) The jacking of individual culvert segment generally causes surface settlement along the tunnel axis longitudinally, with the maximum settlement change reaching 40 mm. The tunnel's transverse section typically exhibits a V-shaped settlement trough profile, with the greatest deformation occurring at the section centre; (2) Ground deformation varies significantly during continuous jacking operation and is influenced by both ground loss and grouting pressures; (3) The pipe roof demonstrates a vertical deformation scale significantly greater (twice as much) than that of the ground surface, underscoring the pipe roof's sensitivity to jacking-induced disturbances, while the surface deformation is mitigated by the pipe roof; (4) The three-dimensional numerical simulation reveals that increasing face pressure is initially more effective for settlement control, the effectiveness plateaus at higher pressures, whereas increasing grouting pressure continues to yield substantial reductions in settlement. These findings contribute to the safety control of EPB culvert jacking combined with PPM for large tunnel construction.

1. Introduction

The culvert jacking method has become one of the most widely utilized tunnelling techniques, particularly for constructing underpass tunnels beneath existing roadways or railways that are sensitive to displacement, as well as for underground pedestrian passages on congested urban streets (Wang et al., 2019; Chen et al., 2021). As a typical non-open-cut tunnelling method, culvert jacking eliminates the need to break the ground surface, thereby minimizing interference with surface traffic and the need to relocate existing facilities, which is a significant technical advantage. Generally, in culvert jacking tunnelling, a series of prefabricated tunnel segments, typically with rectangular cross-sections, are jacked into the ground using specialized hydraulic equipment from a prepared launch shaft (or potentially a surface working pad). This process is conducted while simultaneously excavating and removing the face soil, either manually under an open-face shield or using a closed-

☆ This article is part of a special issue entitled: 'Urban Tunnelling' published in Tunnelling and Underground Space Technology incorporating Trenchless Technology Research.

* Corresponding author.
E-mail address: j.zhang-20@tudelft.nl (J. Zhang).

https://doi.org/10.1016/j.tust.2025.106909
Received 28 February 2025; Received in revised form 15 June 2025; Accepted 14 July 2025
Available online 22 July 2025

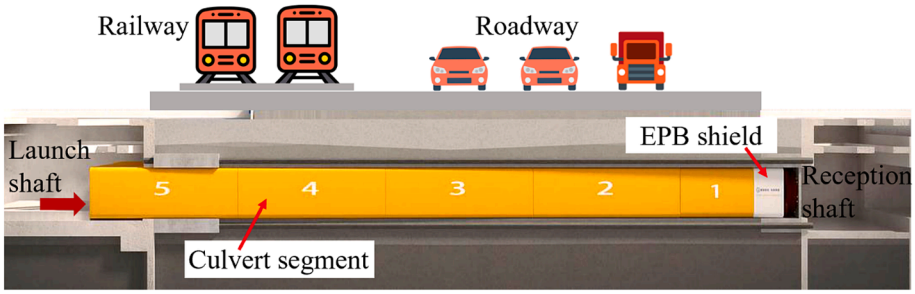

Fig. 1. Schematical view of culvert jacking tunnelling under existing facility.

Table 1
Summary of typical culvert-jacked tunnel projects.

Reference	Tunnel type & location	Dimension (W*H*L, m)	Burial depth (m)	Soil excavation method	Ground improvement
Powderham et al. (2004)	Roadway tunnel under railway, Boston, USA	12*12*240	6.1–7.6	Open face shield	Ground Freezing
Xiao et al. (2005)	Roadway tunnel under urban road, Shanghai, China	34*7.85*125	4.8	Open face shield	Pipe-roof (circumferential)
Pritchard et al. (2011)	Airport highway tunnel under railway, Kent, UK	23*7*126	6	Open face shield	No
Wang et al. (2013)	Roadway tunnel beneath highway, Kaifeng, China	46.8*9.3*52	1.2	Open face shield	Pipe-roof (top edge)
Prakoso and Sabbah (2016)	Culverts under highway, Jakarta, Indonesia	9.7*7.4*93	2	Open face shield	No
Wang et al. (2019)	Underpass beneath highway, Zhengzhou, China	18*6*34.5	2.67	Open face shield	No
Chen et al. (2021)	Utility tunnel under river, Suzhou, China	9.1*5.5*233.6	3.5	EPB shield	No
Zhang et al. (2022)	Subway station under elevated road, Shanghai, China	9.5*4.88*82	4.6	EPB shield	No
Chen et al., (2023)	Underpass beneath roadway, Taipei, China	6.94*4.24*35.6	10.6	EPB shield	Pipe-roof (circumferential)

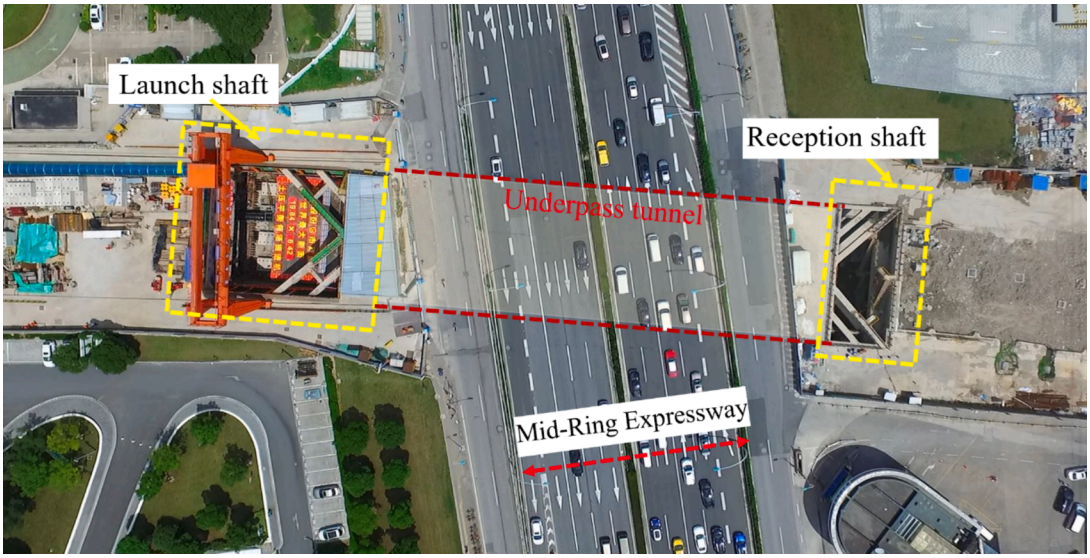

Fig. 2. Bird-view of Tianlin Road Underpass Tunnel project.

face Earth Pressure Balance (EPB) shield machine, as illustrated in Fig. 1 (Bai et al., 2018; Jiang et al., 2022;Li et al., 2024;Jiang et al., 2024). Initially, the culvert jacking method was predominantly employed for constructing tunnels with smaller cross-sections, such as underground pedestrian passages and traffic tunnels in urban areas. However, the recent decade has seen more innovative applications of this technique. For instance, multi-parallel proximity culvert jacking has been utilized to construct multi-lane tunnels (Yang et al., 2016; Hao et al., 2022), while multi-channel close-packed culvert jacking has been applied to create larger underground spaces, such as subway stations (Yang et al., 2022; Wang et al., 2023). It is anticipated that the culvert jacking method will continue playing a significant role in the development of urban underground spaces in the future.

Ground disturbance is a critical safety concern when conducting culvert jacking tunnelling in urban environments. Table 1 provides a brief summary of some representative culvert jacking tunnel projects. These tunnels typically feature a rectangular cross-section, with a burial depth that is less than their width. For example, the large roadway tunnel documented by Wang et al. (2013) has a width of 48 m but a burial depth of only 1.2 m, indicating no ground arching effect. Inappropriate construction measures can easily lead to significant ground deformations or even catastrophic ground collapses during culvert jacking, as evidenced by the severe settlement and face collapse reported by Wang et al. (2013) and Jiang et al. (2023). To mitigate ground disturbance, several prior ground reinforcement measures have been proposed, including initial injective grouting (Kim et al., 2020), ground

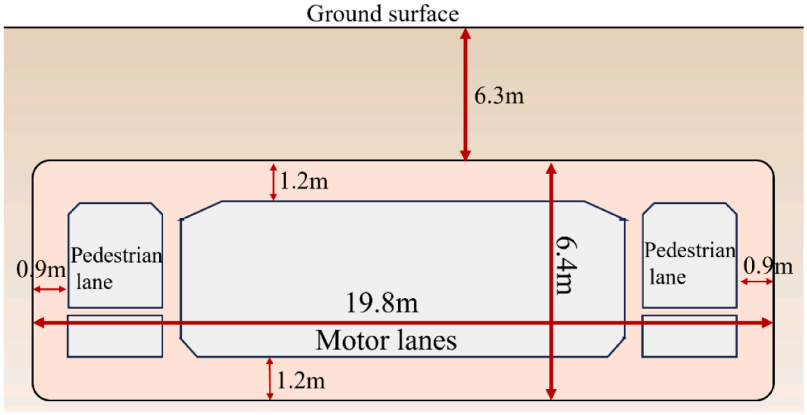

(a) Tunnel cross-section

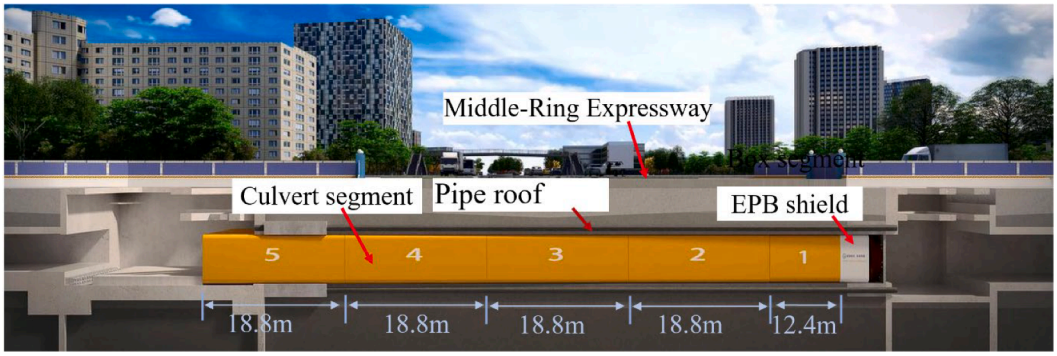

(b) Tunnel longitudinal profile

Fig. 3. Tunnel cross-section and longitudinal profile.

Table 2
Ground strata and geological properties information.

Soil layers	Depth (m)	Unit weight γ (kN/m^3)	Cohesion c (kPa)	Friction angle φ(°)	Water content ω(%)	Constrained modulus E_s(MPa)	Porosity e	Vertical permeability k_v(mm/d)	Horizontal permeability k_h(mm/d)
Silty clay1	2–4	18.5	19	19	32.2	4.46	0.90	0.22	0.71
Muddy silty clay	4–10.2	17.5	12	18	40.6	3.09	1.17	0.32	3.12
Muddy clay	10.2–17	16.8	11	11.5	50	2.20	1.41	0.09	0.13
Silty clay2	17–23	17.9	14	19	35.9	3.79	1.01	0.29	1.05
Silty sand1	23–29	18.5	5	31	29	9.43	0.85	13.5	22.1
Silty sand2	29–32	19.5	39	19	21	6.5	0.71	0.89	0.13
Sandy silt	32–40	18.9	3	33	27	10.9	0.78	11.8	19.5

freezing (Powderham et al., 2004), and the pipe-roof preconstruction method (PPM). Among these, PPM offers advantages in terms of ensuring effective ground reinforcement while balancing costs. Typically, PPM involves constructing a dense pipe corridor, or pipe roof, along the external tunnel circumference prior to pipe jacking construction. To enhance the interconnection of adjoining pipes and improve waterproof reliability, the dense pipe roof is generally fitted with special socket connections and installed along the tunnel's full circumference, forming an enclosed pipe array. In recent decades, PPM has gradually evolved into a crucial auxiliary ground pre-reinforcement technique for large culvert jacking tunnelling projects (Niu, 2019; Xie et al., 2019).

Previous studies have examined the application of the PPM for constructing shallow underpasses, primarily in conjunction with the New Austrian Tunnelling Method (NATM). For example, Yang et al. (2020a, b) analysed ground deformation and jacking force characteristics during the installation of pipe arrays for an underpass tunnel beneath a railway station. Zhang et al. (2016) investigated movement and installation errors associated with pipe roof installation in the Gongbei Tunnel project, while Jia et al. (2020) studied ground deformation induced by the jacking of a dense pipe roof as pre-support before the excavation of a large underground subway station. In the research conducted by Lu et al. (2023), the bearing capacity of pipe-filled concrete slab linings was experimentally assessed. Previous studies demonstrate the effectiveness of PPM in constructing underground structures using NATM method. However, it is noteworthy that early studies have predominantly focused on ground deformation and jacking forces during the pipe installation process, with less attention on the ground response during subsequent tunnel excavation.

In addition to the NATM tunnelling, the integration of PPM with culvert jacking tunnelling has also been explored previously. For instance, He et al. (2022)examined the postures and errors associated with pipe installation in a box culvert jacking project, while Tang et al.

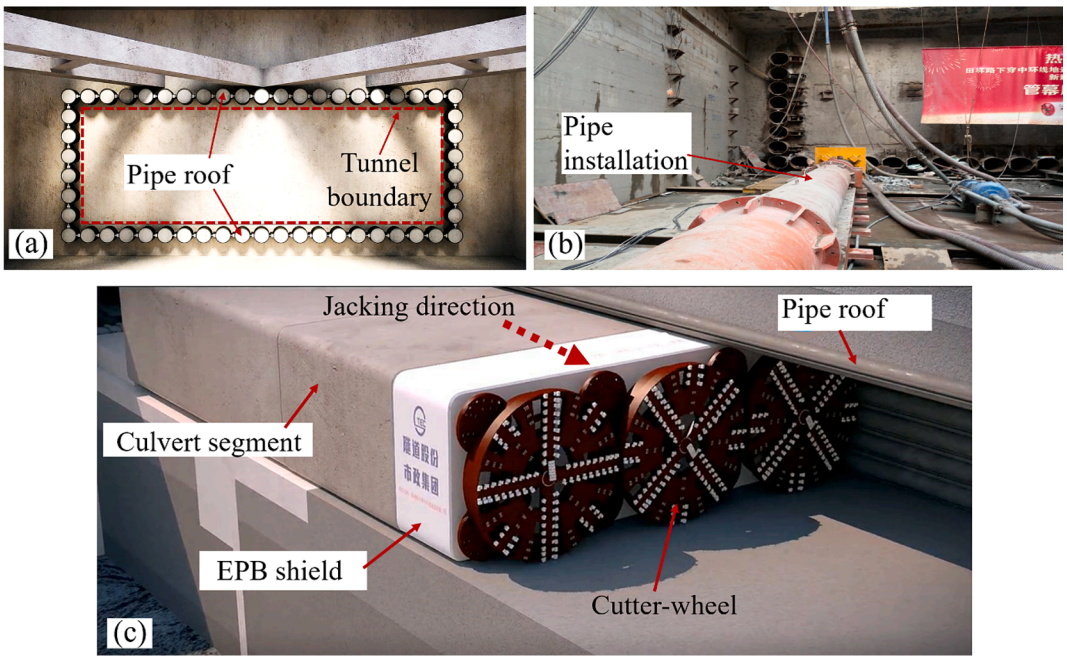

Fig. 4. Schematic of work procedure:(a) Pipe roof boundary;(b) pipe roof installation and (c) EPB culvert jacking.

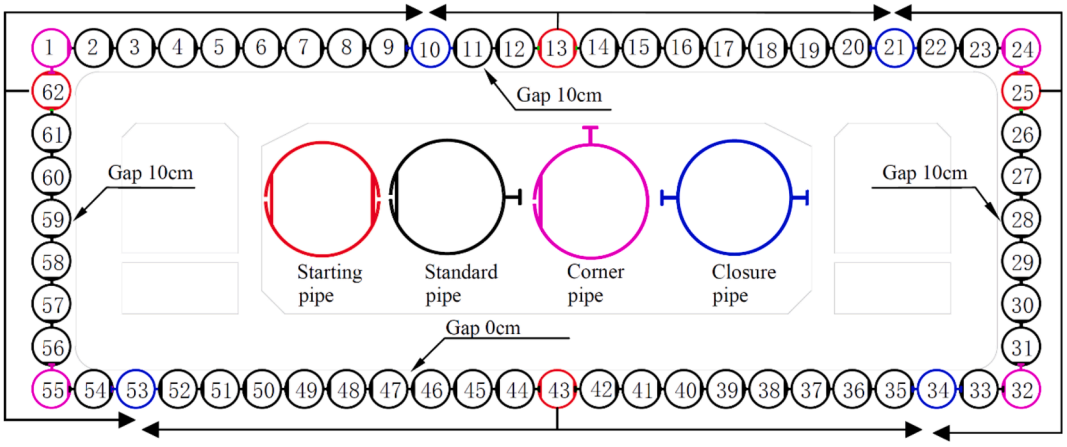

Fig. 5. Layout of pipe roof and installation sequences.

(2022) analysed the ground deformations during pipe roof construction. Xie et al. (2019) evaluated the effectiveness of pipe roof in stabilizing the excavation surface during culvert jacking through numerical simulation. Furthermore, Xiao et al. (2005) and Wang et al. (2013) investigated ground deformation during the culvert jacking process using an open-face steel grid extrusion (SGE) shield in combination with PPM. However, there are very few studies on the deformation response of EPB culvert jacking tunnelling. As indicated in Table 1, there is a growing trend towards the use of full-face mechanized EPB shields rather than open-face SGE shields. The combination of the PPM with EPB culvert jacking presents a promising solution for urban shallow tunnelling, particularly in soft ground conditions. Notably, the technical knowledge of it remains largely unexplored, primarily due to a lack of project case studies and insufficient field monitoring data.

To address existing knowledge gaps, this study specifically examines the ground disturbance characteristics associated with EPB culvert jacking tunnelling combined with pipe-roof preconstruction method (PPM). The investigation is based on an urban road underpass tunnel project in mainland China, featuring the largest cross-section to date (19.8 m in width and 6.4 m in height) constructed in soft ground. The deformation time-history of both ground strata and pipe roof is meticulously recorded via comprehensive monitoring throughout the culvert jacking process, followed by a three-dimensional numerical simulation. In the remainder of this study, Section 2 introduces the background engineering information and details the construction process, while Section 3 presents and analyses the ground surface deformations as well as the pipe roof deformations throughout the culvert jacking process. To further explore the impacts of face support pressure and lubrication grouting pressure on ground deformation, a three-dimensional numerical simulation is conducted in Section 4, accompanied by proposed technical recommendations, and Section 5 concludes the study. The findings from this study contribute to advancing the application of EPB culvert jacking with PPM for large tunnel construction.

2. Background engineering

2.1. Project information

The Tianlin Road Underpass Tunnel features an urban road tunnel constructed beneath the Middle-Ring Expressway in Shanghai, China. As

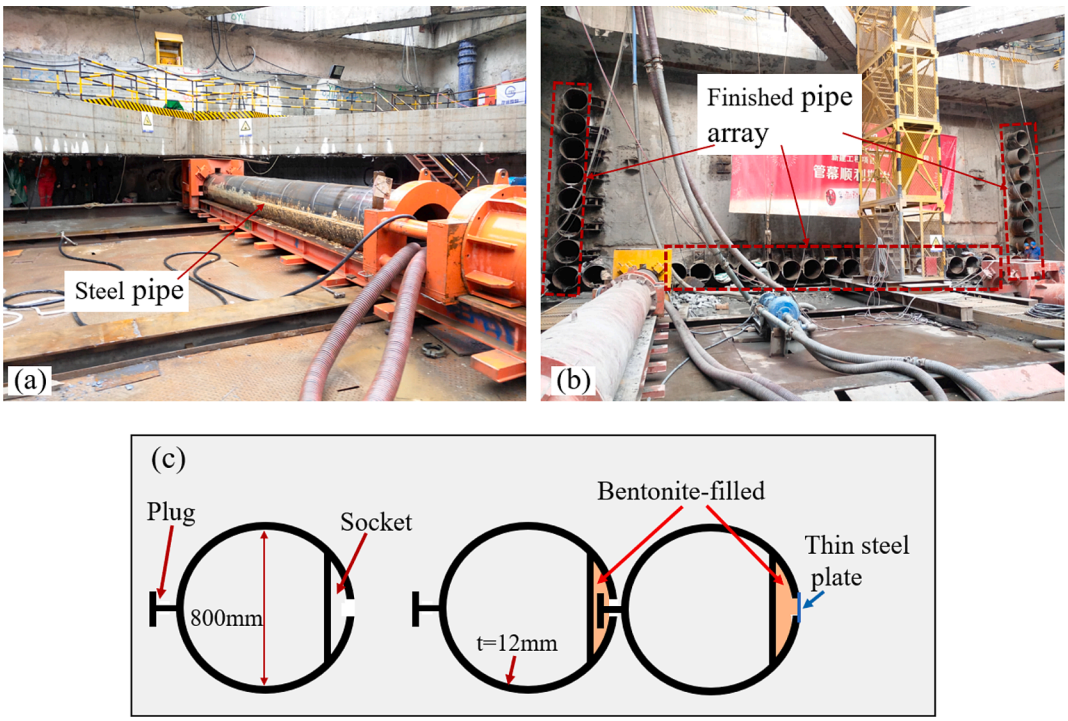

Fig. 6. Pipe-roof preconstruction on the site: (a) pipe jacking (b) finished pipe array and (c) inter-pipe connection.

Table 3
Box culvert jacking process.

Segment No.	Construction period	Duration (days)	Distance of head to the launch shaft (m)
1	Jul. 13 – Jul. 19, 2018	7	13.3
2	Aug. 16- Aug. 26, 2018	11	32.6
3	Sep. 17- Sep. 21, 2018	5	51.4
4	Oct.12 – Oct.15, 2018	4	70.2
5	Nov. 23 – Nov. 26, 2018	4	82

the expressway serves as a major urban transportation artery, it is required that underpass tunnel construction does not disrupt traffic flow or interfere with utilities above ground (see Fig. 2). The whole underpass tunnel extends approximately 696 m long, and the section beneath the expressway has a burial depth of 6.2 m covering about 100 m longitudinally. Given the impracticality of large-scale open trenching excavation, the earth pressure balanced (EPB) culvert jacking method is selected for building this tunnel.

Considering the very weak soft ground and small burial depth, pipe-roof preconstruction is implemented to pre-support the ground and serve as a water barrier, ensuring the safety of the subsequent culvert jacking and mitigating soil disturbance caused by groundwater movement. As shown in Fig. 3(a), the jacked tunnel has external dimensions of 19.8 m in width and 6.4 m in height, accommodating three motor

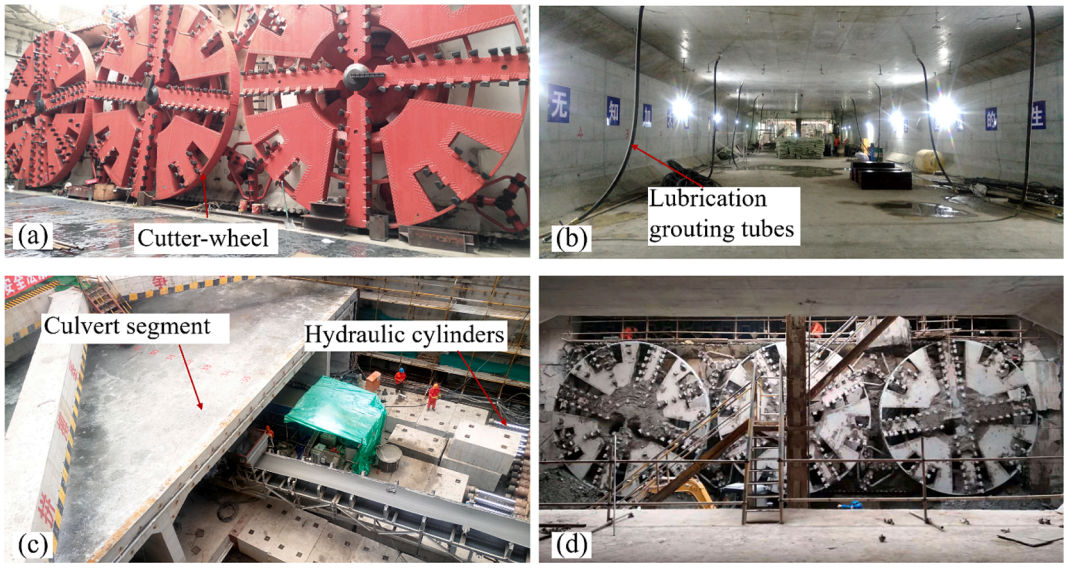

Fig. 7. Culvert jacking process: (a) EPB shield before launch (b) internal view (c) culvert being jacked (d) reception of the EPB shield.

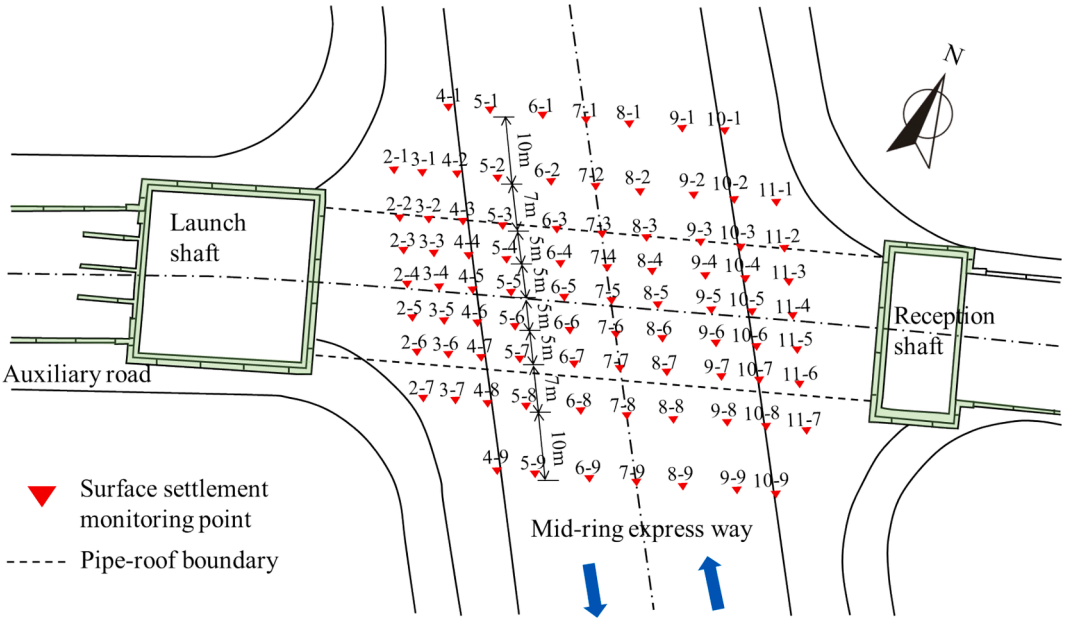

Fig. 8. Layout of monitoring points on surface.

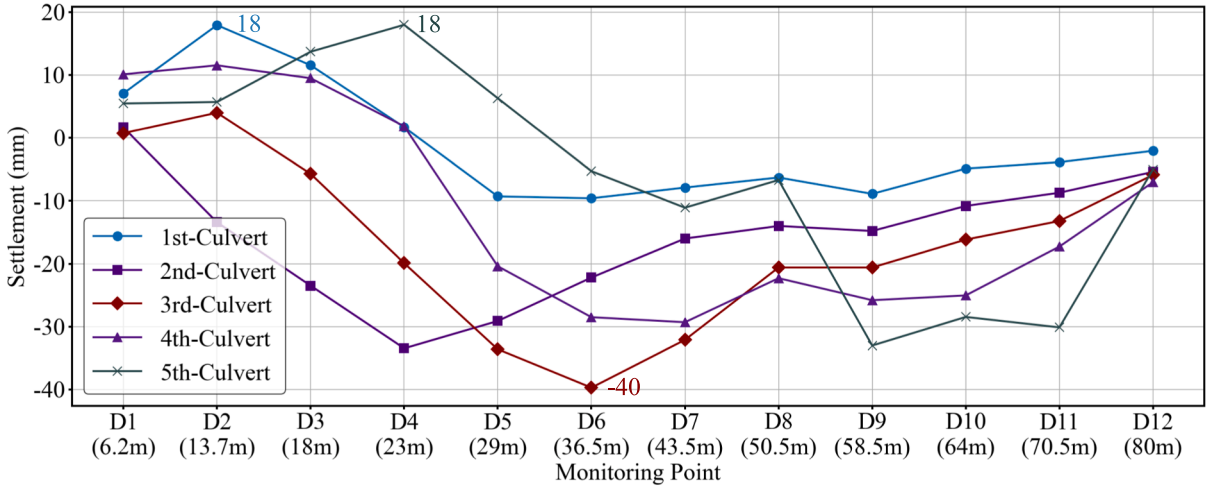

Fig. 9. Surface settlement changes at central line with each culvert jacking.

lanes in the centre and two pedestrian lanes on each side. Longitudinally the jacked section consists of five culvert segments, with a total length of 84.6 m (see Fig. 3(b)).

2.2. Geological conditions

The tunnel has a burial depth of around 6.2 m, with geological strata comprising highly plastic and compressible mucky silty clay. The typical ground profile along with soil properties are presented in Table 2. Within the revealed depth, ground strata at the tunnelling site stems from Quaternary deposits of estuarine, coastal, shallow sea and marsh facies, which are composed of mainly clayey and sandy soil. From top down, the ground strata include backfills, silty clay, muddy silty clay, clayey sands et al., as listed in Table 2. The observed long-term phreatic water level was about 1 to 1.5 m below the ground surface. It should be noted that strata crossed by the pipe-roof (ranging from 7 m to 14 m below ground surface) are the muddy silty clay and the muddy clay which both possess very weak strength and high deformability. Therefore, a delicate and cautious control of the culvert jacking process should be conducted to mitigate ground deformations.

2.3. Culvert jacking tunnelling combining with PPM

2.3.1. General tunnelling process description

In this project, a super large EPB shield machine (19.5 m wide and 6.4 m high) is deployed. Compared with manual excavation using steel extrusion grids (SEG) shield as in previous culvert jacking project (Xiao et al., 2005), the EPB shield is more effective in ground disturbance control and labour-saving. The general construction process of this project is explicitly described as follows: (1) Building the launch shaft and reception shafts, which will serve as the work platform for subsequent pipe roof installation and concrete culvert segment fabrication (in Fig. 4(a)); (2) Pipe roof installation using normal pipe jacking method (see Fig. 4(b)). Custom-made steel pipes are successively jacked into the ground horizontally, extending through the whole jacking length from the launch to the reception shafts, and the finished pipe rows forms a stable roof along the tunnel's circumference (see Fig. 4(a)); (3) Box culvert jacking. After the pipe umbrella is completed, a head EPB shield

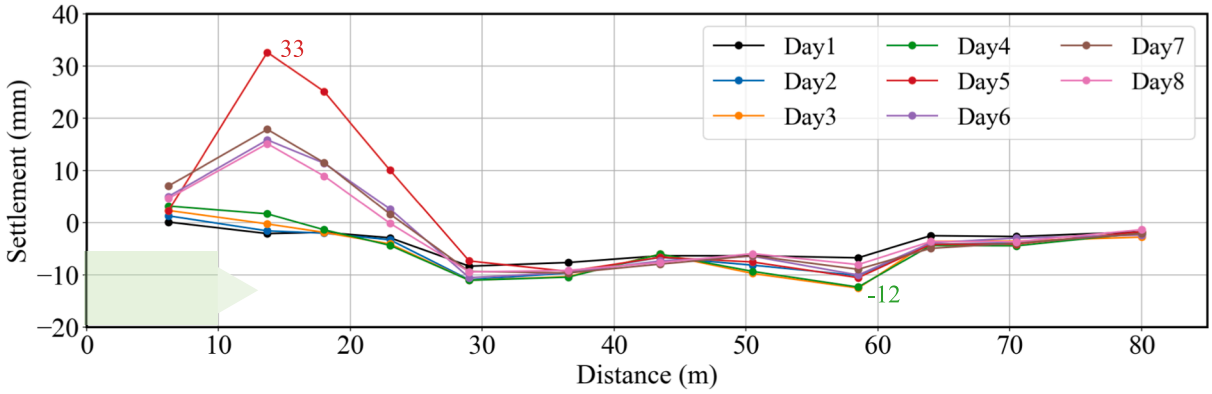

(a) 1st culvert segment jacking

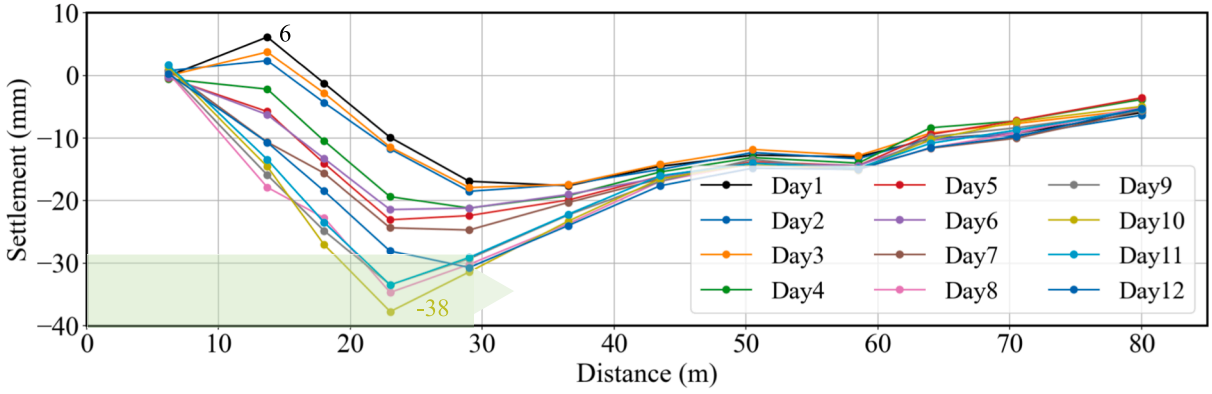

(b) 2nd culvert segment jacking

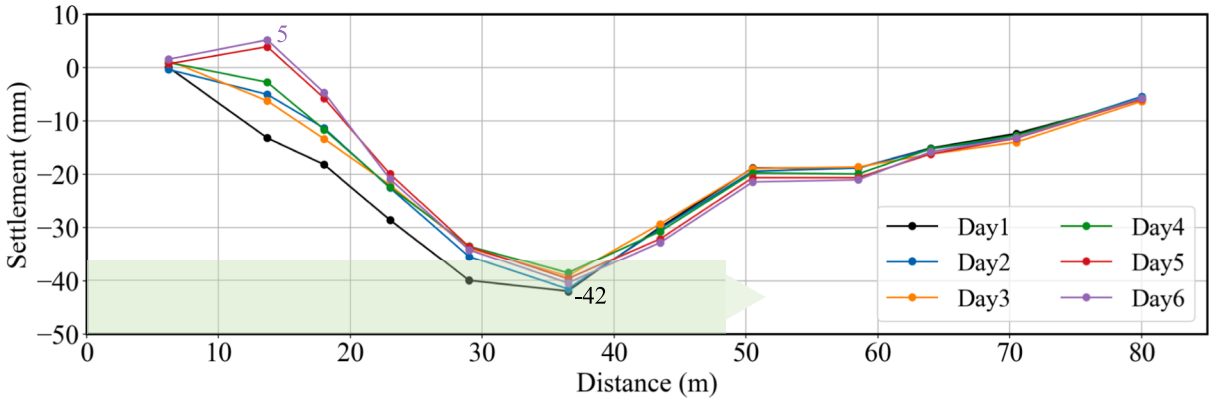

(c) 3rd culvert segment jacking

Fig. 10. Surface settlement during each culvert segment jacking.

is assembled in the launch shaft, followed by the concreting and curing of the first culvert segment. Hydraulic cylinders, positioned against the reaction wall, push the segment and shield forward and penetrating the ground, while excavation and soil removal occur in parallel with the jacking of each culvert segment (in Fig. 4(c)). This culvert casting and jacking process is repeated successively until the shield reaches the reception shaft, completing the designated tunnel.

2.3.2. Pipe-roof preconstruction method (PPM)

The pipe roof is constructed by thrusting individual steel pipe into the ground successively using normal pipe jacking method (Figs. 5 and 6). Notably, the new inter-pipe connection consisted of an external plug and an embedded socket as shown in Fig. 6(c). The socket void is initially filled with bentonite clay to waterproof the socket prior to pipe jacking, and the small cutout is temporarily sealed with a very thin steel plate by spot welding.

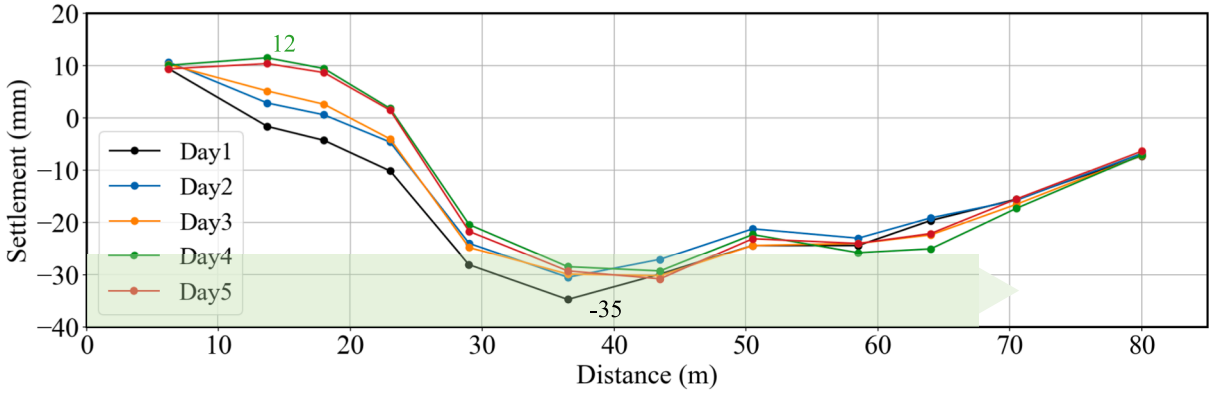

(d) 4th culvert segment jacking

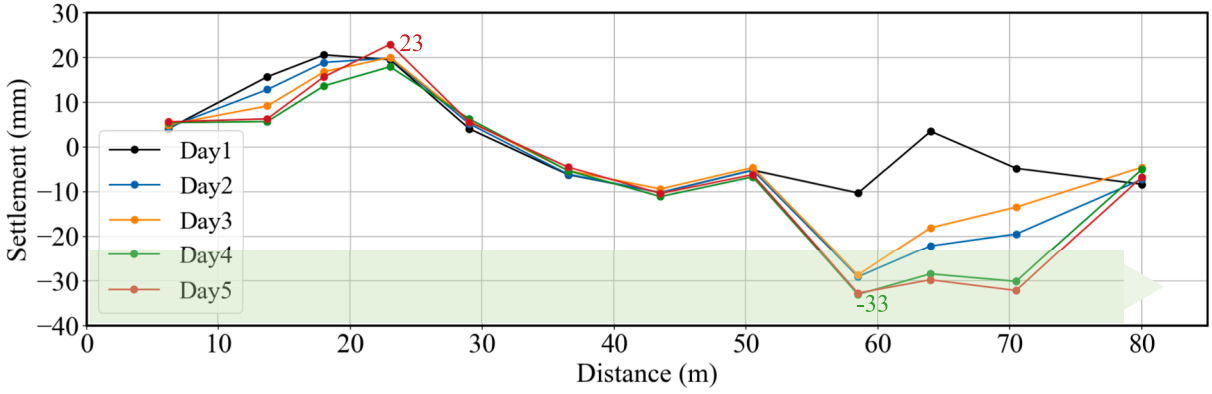

(e) 5th culvert segment jacking

Fig. 10. (*continued*).

Four N800 slurry type pipe jacking machines with a length of 3.6 m each were used to jack a total of 62 steel pipes, each with an inner diameter of 800 mm and thickness of 12 mm. The layout and installation sequence of the pipe roof are shown in Fig. 5 below, and the top of the pipe roof locates only 6.3 m below ground surface. The spacing between the pipes was 81 mm horizontally on the top and bottom pipe rows, and 92 mm vertically in the left and right pipe rows. Four types of pipe cross-sections were used: starting pipes, standard pipes, corner pipes, and closure pipes. The pipe jacking process usually begins with the starting pipe and ends with the closure pipe. Each 86 m-long pipe is formed by welding the ends of seven shorter pipe sections together, the first of which was inserted into the ground at a length of 14 m, while the remaining six segments were 12 m in length. To increase the stiffness of the pipe roof, 55 were filled with low-strength concrete, while the remaining seven hollow pipes were left unfilled to serve as channels for monitoring vertical deformations.

The entire duration of continuous jacking of the pipe roof totalled 164 days. According to the analysis of on-site measurement data, for the top and bottom pipe rows, 86.8 % of the monitoring points had a horizontal deviation of less than 4 cm, and 91.7 % had a vertical deviation of less than 4 cm. For the left and right pipe rows, 98.4 % of the monitoring points deviated horizontally within 4 cm and 89.6 % deviated vertically within 4 cm (He et al., 2022). Thus, the plug-socket inter-pipe connections can provide a significant constraining effect thereby reducing the trajectory error. However, there were also a small number of pipes that showed significant deviations at some of the monitoring locations after jacking was completed, with the largest horizontal deviation reaching 8.64 cm and the largest vertical deviation reaching 11.05 cm. Throughout the jacking process, the maximum ground settlement monitored reached 89 mm, and the maximum uplift deformation was about 85 mm (Tang et al., 2022). After the completion of the pipe-roof preconstruction, the first concrete culvert segment was subsequently fabricated in the launch shaft and further jacked.

2.3.3. *Culvert jacking tunnelling*

The entire jacked tunnel is divided into five culvert segments longitudinally, and the construction durations and jacking distance of each segment are shown in Table 3. Fig. 7 displays the general culvert jacking process that counts to a total of 5 months. During culvert jacking, the EPB shield excavates the front face while the muck is discharged via a preliminary screw conveyor and further long-range covey belt as shown in Fig. 7 (c). Synchronous lubrication grouting is injected into the circumference of the tunnel to reduce the interface frictions. Ground deformations and pipe movements are monitored specifically throughout the tunnelling process.

3. Field monitoring Investigations

To monitor the surface settlement throughout the culvert jacking, a total of 98 monitoring points is pre-arranged to distribute on 12 arrays on the surface of Middle-Ring Expressway (as shown in Fig. 8). Of the 12 arrays, seven (arrays 4–10) are within the expressway boundary, with nine monitoring points on each array, and the other five arrays (arrays 1–3, 11, 12) are set on the auxiliary road area, with seven monitoring points on each array. During culvert jacking process, the monitoring frequency is twice per day.

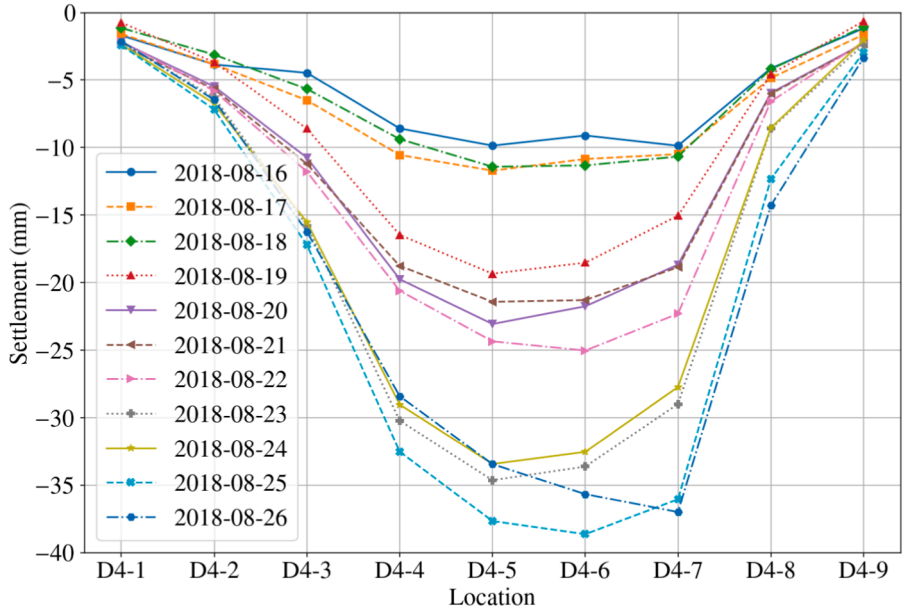

(a) D4 transverse cross-section (23m to launch shaft)

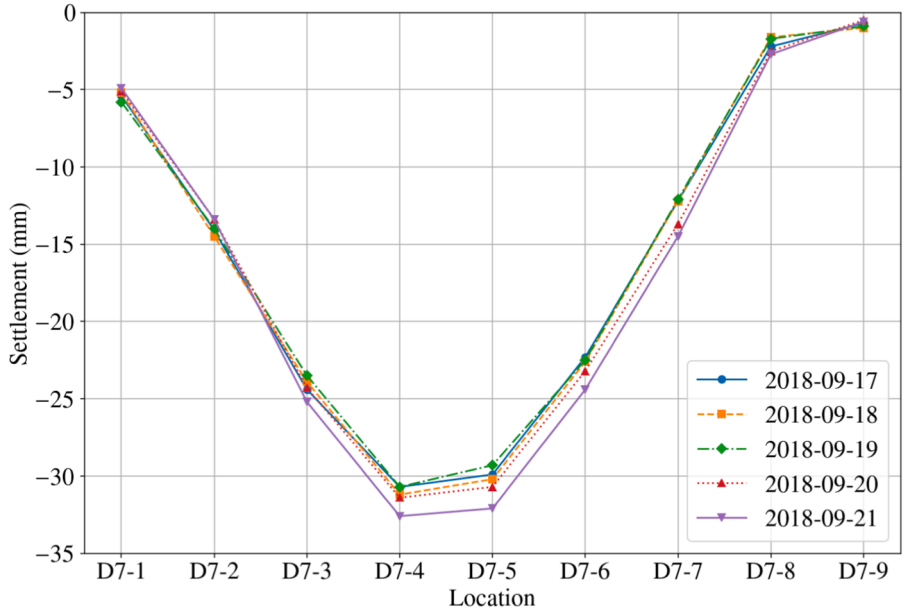

(b) D7 transverse cross-section (43.5m to launch shaft)

Fig. 11. Ground deformation of three selected transverse cross-sections.

3.1. Ground deformation monitoring

3.1.1. Longitudinal ground surface deformation along tunnel axis

The changes of ground settlement along the central axis between the start and completion of each culvert segment jacking are plotted in Fig. 9. Note that the recorded settlement at the completion is baselined at the start of this segment jacking. When the 1st culvert jacking is completed (13.3 m from launch shaft), the ground surface shows a significant heave in length between monitoring points D1 and D4 (23 m) and a different degree of subsidence after D4. The largest heave occurs at D2 (13.7 m) reaching 18 mm, while the largest settlement occurs at D6 (36.5 m) and reaches −10 mm. All the monitoring points along the central line experience subsidence during the 2nd culvert jacking, with D4 (23 m) reaching a maximum of −33 mm. Furthermore, the surface settlement pattern during the 3rd culvert jacking is similar to that of the 2nd one, with the maximum settlement occurring at the mid-point of the jacking length (D6, 36.5 m), and smaller settlements near the launch and reception shafts.

After the jacking of the 4th and 5th culverts, the ground surface in the area close to the launch shaft exhibits a heave movement (namely, the cumulated subsidence in the previous construction is mitigated), but within the length where the face excavation is carried out (51.4 m-82 m), there is a continuous subsidence of the ground surface. For instance, at the completion of the 4th culvert, there appears an uplift in the range

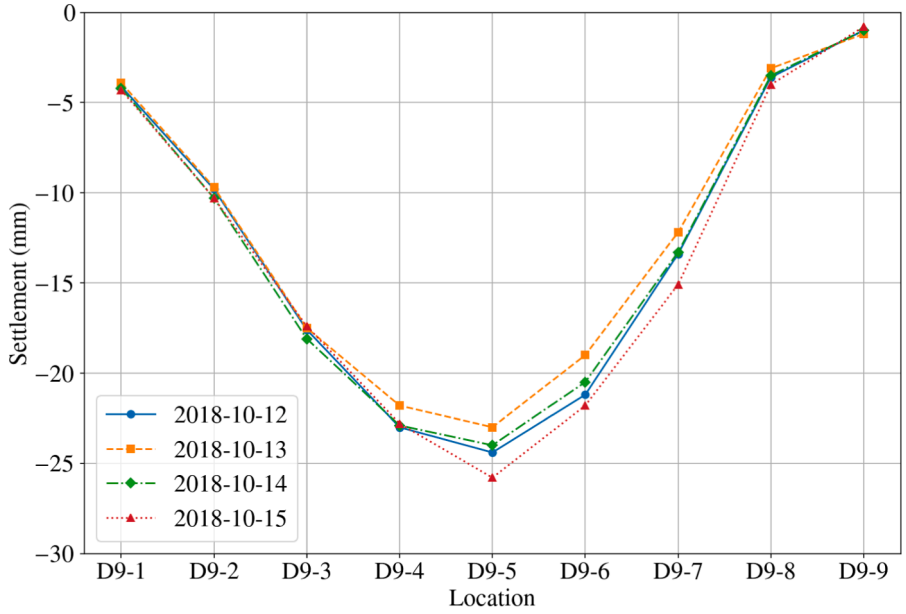

(c) D9 transverse cross-section (58.5m to launch shaft)

Fig. 11. (*continued*).

from 6.2 m to 29 m, with a maximum of 11 mm at 13.7 m, while the maximum subsidence is −29 mm at 43.5 m. After the jacking of the 5th culvert, a maximum heave of 18 mm is measured at 23 m, while the maximum subsidence is –33 mm (at 58.5 m). It can be observed that at the completion of each culvert jacking, the maximum ground deformation typically does not occur at the front cutterhead location. For example, after the jacking of the 2nd culvert, the excavation face is at 32.6 m, while the maximum subsidence occurs at 23 m. This phenomenon will be discussed in more detail in the next section.

To further analyse the characteristics of surface settlement in short term, Fig. 10 plots the daily settlement variations measured during the jacking of individual culvert segments. The starting day of each culvert jacking is named as day 1, and the accumulated surface deformations (relative to day 1) in the subsequent days are recorded. In Fig. 10(a), during the 1st culvert jacking, surface deformation at the monitoring point D2-4 (13.7 m to the launch shaft) reaches a maximum heave of 32 mm on the 5th day, then it further decreases as the cutterhead approaches this location. Fig. 10(b) records a highlighted subsidence during the 2nd culvert jacking, with the maximum subsidence occurring on the 10th day, reaching about −38 mm, followed by a slight recovery subsequently. Fig. 10(c) and 10(d) show that during the jacking of the 3rd and 4th culverts, the surface experiences less than −5mm of subsidence, with a partial recovery at completion. Fig. 10(e) shows a gradual surface subsidence during the jacking of the 5th culvert, with a maximum of –32 mm. Except for the 5th culvert jacking, the maximum deformation occurs during the jacking process, which contrasts with the 5th culvert where maximum deformation occurs at the completion of jacking. This might be due to the variation of lubrication grouting pressures and soil's elastic deformation recovery after cutterhead passing through.

3.1.2. *Transverse cross-section ground deformation*

Fig. 11 shows the deformation time-history of three monitoring arrays (D4, D7, D9) during the culvert jacking, corresponding to three transverse cross-sections. The selected cross sections are located at 23 m, 43.5 m, and 58.5 m distance to the launch shaft (see Fig. 9). Therefore, the ground deformations during the shield cutterhead approaching, passing through, and leaving the monitoring cross-section are specifically recorded.

Fig. 11(a) illustrates the deformation variation at transverse section D4 during the jacking of the 2nd culvert segment (from 2018 to 08-16 to 2018–08-26). The deformation pattern indicates a typical V-shaped subsidence trough similar to that induced in general circular shield tunnelling, with the maximum subsidence occurring between locations D4-4 and D4-7, and the deformation at the centreline (D4-5) being the most significant, with a settlement of −6 mm recorded in just one day (from 08 to 18 to 08–19). The maximum subsidence during the whole jacking process reaches approximately −38 mm, indicating that the soil above the culvert experiences the greatest disturbance. Over the monitoring period, the subsidence tends to be more significant gradually. On the final day of jacking, a partial rebound in subsidence is observed; however, it is not uniform across the entire transverse section. The rebound at the centreline (D4-5) reaches 5 mm, while at the edge of the culvert (D4-7, 10 m from the centreline), a subsidence of −1 mm is still recorded. This is probably a result of grouting operations conducted near the end of the jacking process, which causes partial but not uniform uplifting over the cross section.

Fig. 11(b) illustrates the deformation variation at monitoring section D7 during the jacking of the 3rd culvert segment (2018–09-17 to 2018–09-21). The cross section shows a more significant V-shaped deformation pattern, but the trough is biased to exhibit a sharply concentrated settlement at points D7-4 (5 m from the centre line) and D7-5 through the whole jacking process. The overall variation trend across the monitoring section is consistent, with the maximum change occurring at the central point D7-5, with a gradual subsidence range of about 2.5 mm from day 1 to day 4. The maximum daily subsidence variation occurs on the final day, with a surface subsidence of 2 mm observed. This subsidence extends across a range of 15 m (from D7-3 to D7-6), nearly covering the entire culvert width, which highlights the significant impact of the cutter head's passage on surface ground.

Fig. 11(c) shows the settlement changes at monitoring section D9 during the jacking of the 4th culvert segment (2018–10-12 to 2018–10-15). The overall section formed a nearly symmetrical V-shape centred around D9-5 (the tunnel centreline). The largest deformation during the construction occurs near the centre point. On the second day of construction, as the cutterhead approaches the monitoring point, an uplift

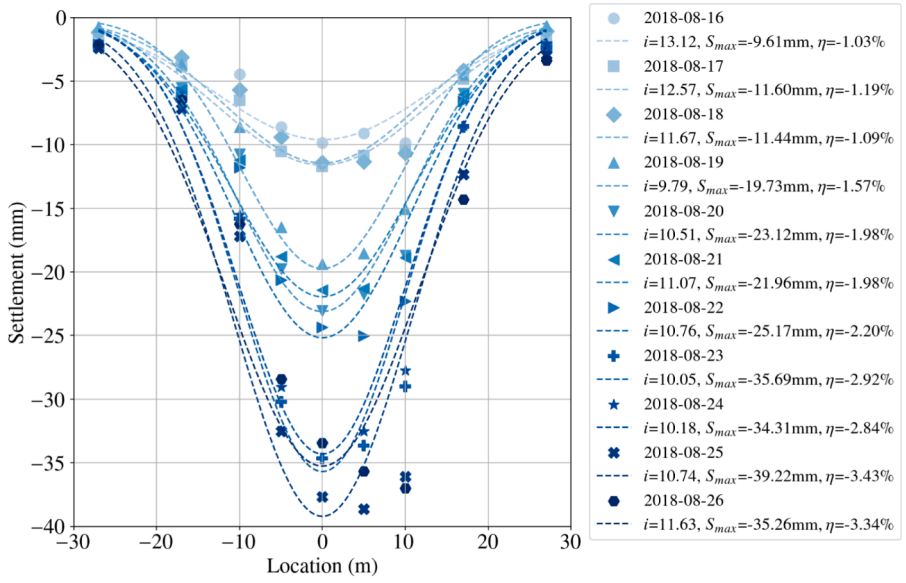

(a) D4 transverse cross-section (23m to launch shaft)

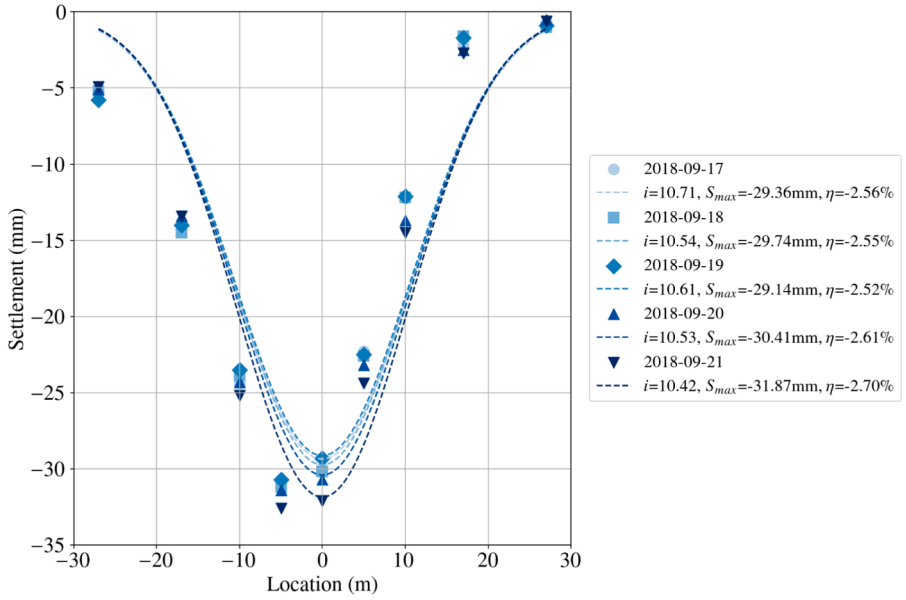

(b) D7 transverse cross-section (43.5m to launch shaft)

Fig. 12. Gaussian curve fits and soil volume loss of transverse sections.

of 1.9 mm is observed at D9-5. This uplift effect gradually decreases from the centreline toward the two sides, nearly covering the entire culvert width. Over the following two days, as the cutter head passed through and moves away from the monitoring point, the surface settles to its initial value and this tendency continues further. On the final day a large subsidence occurs at D9-5, reaching about −2 mm. Besides, the scale of maximum settlement at D9 is slightly smaller than those at D4 and D7.

Transverse settlement profiles provide valuable insights into the extent of ground volume loss associated with the culvert jacking process. Based on the approach proposed by Peck (1969), surface settlement is assumed to occur under undrained conditions, whereby the volume of the settlement trough corresponds directly to the volume of ground loss. Furthermore, the surface settlement trough is typically modelled as following a Gaussian distribution. Consequently, the transverse surface settlement can be estimated using the following equations:

$$S(x) = S_{\max} e^{-\frac{x^2}{2i^2}} \tag{1}$$

$$S_{\max} = \frac{V_S}{i\sqrt{2\pi}} \tag{2}$$

$$V_S = \eta \pi R^2 \tag{3}$$

where $S(x)$ represents the surface settlement at a horizontal distance x from the tunnel centerline; $S_{\max}$ is the maximum surface settlement above the tunnel axis; V_S is the volume loss per unit length of soil longitudinally; i is the settlement trough width parameter, η is the

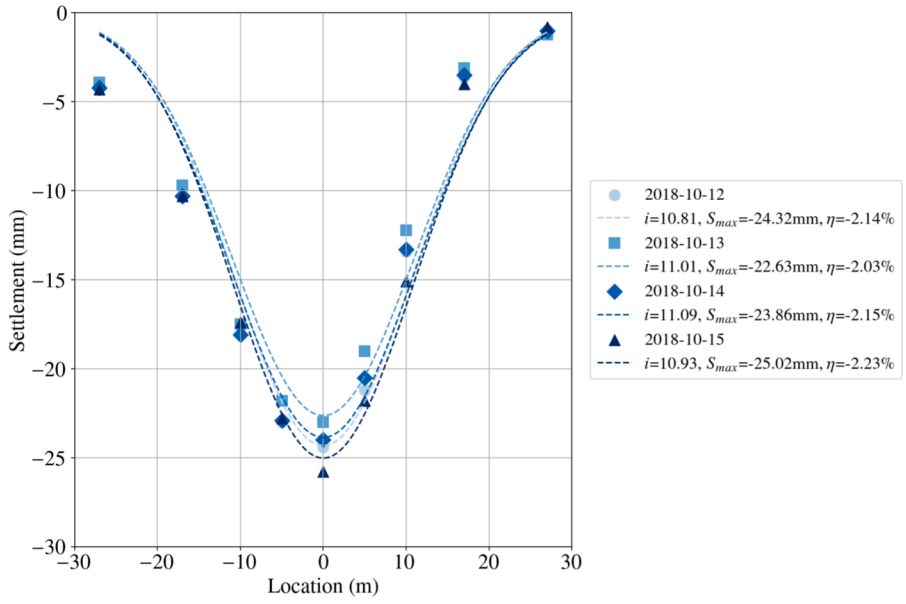

(c) D9 transverse cross-section (58.5m to launch shaft)

Fig. 12. (*continued*).

ground loss ratio; and D_e is the equivalent diameter of the culvert cross-section. The surface settlement data from the three cross sections shown in Fig. 11 are fitted using this model, and the curve patterns with key parameters are presented in Fig. 12.

Based on the fitting results, the ground loss ratio at cross section D4 exhibits considerable fluctuations throughout the entire pipe jacking process, with an overall increasing trend as the cutterhead advances. The ground loss ratio reaches a peak value of −3.43 % on the penultimate day of jacking, before slightly decreasing to −3.34 % on the final day. In contrast, the ground loss ratios at the other two cross sections, D7 and D9, display minimal variation, ranging from −2.52 % to −2.70 % and −2.03 % to −2.23 %, respectively. During the jacking of the second culvert, excessive grouting was implemented between August 24 and August 26, which appears to have effectively inhibited further increases in the soil loss rate. The comparatively lower soil loss ratios observed during the jacking of the third and fourth culverts can be primarily attributed to improved grouting practices employed during these stages.

3.1.3. *Time-series data of individual ground monitoring points*

The time-history of surface deformation at five selected monitoring points D1-4, D4-5, D7-5, D10-5, and D12-4 throughout the entire culvert jacking period are demonstrated specifically in Fig. 13. Note that these five points correspond successively to the middle of the jacking length of each culvert. In general, it can be observed from Fig. 13 that the passage of the shield cutterhead often causes significant deformation fluctuations at that point. In contrast, the impact on points farther from the cutterhead is much smaller. For example, as shown in Fig. 13(a), during the jacking of the 1st segment, the daily deformation at the point D1-4 ranges between 2 to 3 mm, whereas the deformation variation at other points farther (from the excavation face) is much less noticeable, with daily variations generally fluctuating within ± 1 mm. Similarly, in Fig. 13(b) during the jacking of the 2nd segment, significant deformation is primarily observed at monitoring point D4-5, where the daily subsidence recorded during the passage of the cutterhead reaches −10 mm. This indicates that the instantaneous disturbance to the soil induced by cutterhead is mainly concentrated near the excavation face.

The ground deformation observed at the first three monitoring points demonstrates a recoverable pattern throughout the jacking process, as illustrated in Fig. 13(a)-(c). For example, at monitoring point D1-4, the maximum heave deformation recorded during jacking is 12 mm; however, this deformation nearly returns to zero upon completion of the entire jacking operation. Similar trends are observed at monitoring points D4-5 and D7-5, where surface deformation gradually rebounds during subsequent culvert jacking activities. In contrast, monitoring points D10-5 and D12-4 exhibit permanent subsidence. By the conclusion of the jacking process, the subsidence at D10-5 and D12-4 reaches −38 mm and −21 mm, respectively. This persistent subsidence is likely attributable to irreversible soil disturbances induced during the construction process.

Furthermore, lubrication grouting pressures can induce substantial ground uplift. As illustrated in Fig. 13(a)-(c), beginning around October 2018, monitoring points D1-4, D4-5, and D7-5 exhibit a pronounced upward trend in cumulative deformation (i.e., a reduction in subsidence), with the most significant change of 45 mm observed in Fig. 13 (b) during the jacking of the second culvert segment. This uplift is attributed to lubrication grouting applied to the top roof of the completed culvert segments between September 26, 2018, and October 5, 2018. These findings suggest that regulating grouting pressure during the culvert jacking process can effectively mitigate soil disturbance and deformation in real time. However, subsidence resumes once the grouting pressure is reduced. As shown in Fig. 13(a) and (b), even after the completion of the fifth culvert jacking, notable deformation continues to develop when lubrication grouting is replaced by cementitious backfilling.

3.2. *Pipe roof deformation*

Vertical deformations of four steel pipes (S5, S11, S14, S20 in Fig. 5) at the top array are recorded after the completion of each culvert jacking. In Fig. 14, the red vertical lines mark the cutterhead position at the completion of each culvert jacking. By the completion of the first culvert jacking (with the cutterhead positioned at 13.3 m), all four pipes exhibit upward movement, with the maximum heave reaching 30 mm, which slightly exceeds the maximum surface uplift of 18 mm observed in Fig. 9. Upon completion of the second culvert jacking, pipe S20 displays settlement along the entire monitored section, with a maximum value of approximately −30 mm. In contrast, the remaining three pipes demonstrate a pronounced longitudinal flexural deformation pattern:

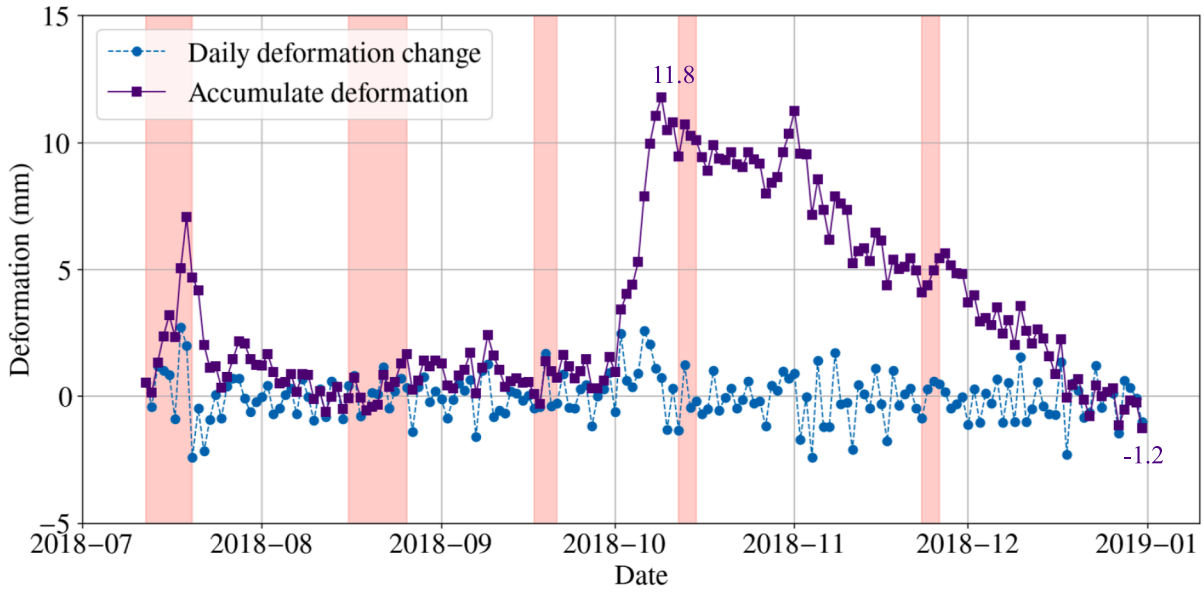

(a) D1-4 (6.2m)

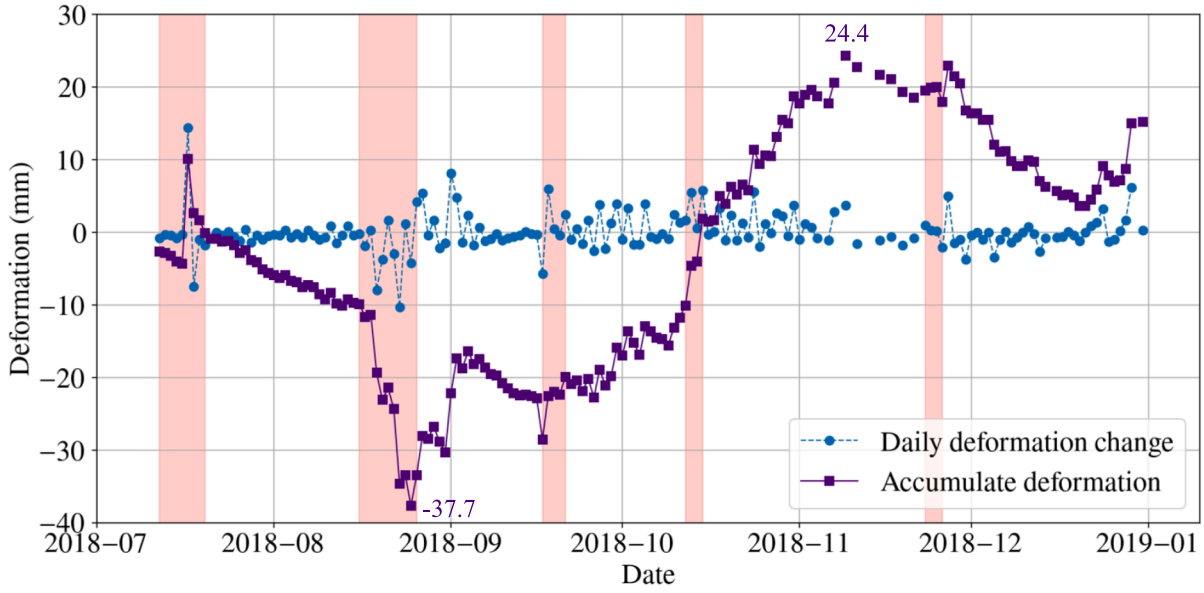

(b) D4-5(23m)

Fig. 13. The deformation time-history of five characteristics monitoring points.

heave is observed at the far end behind the cutterhead, while significant settlement occurs near the cutterhead. This flexural deformation pattern persists following the completion of the third and fourth culvert jackings, with portions of the pipe length exhibiting substantial heave and other sections experiencing settlement. Finally, at the conclusion of the fifth culvert jacking, the maximum uplift of 216 mm is recorded at pipe S11.

Although localized subsidence occasionally occurs along the pipes, continuous grouting throughout the jacking process predominantly results in an overall upward displacement of the pipe roof. By the completion of jacking, the entire pipe roof has been elevated by approximately 100 mm relative to its initial position at the start of construction, effectively limiting surface subsidence to within –32 mm. Furthermore, the magnitude of deformation observed in the four pipes is substantially greater than that recorded at the ground surface.

To further compare the deformation scale of pipe roof and ground surface, the pipe S11 deformation and surface settlement monitored at the completion of each culvert jacking is shown in Fig. 15. It is evident that the pipe predominantly exhibits heave deformation pattern, whereas the surface mostly exhibits a subsidence except at 1st culvert jacking. As shown in Fig. 15(b), when pipe S11 shows a maximum heave of 55 mm, the corresponding surface settlement is around −30 mm. Similarly, Fig. 15(d) illustrates that after the completion of the 4th culvert jacking, pipe exhibits a significant heave at 0–60 m, with a

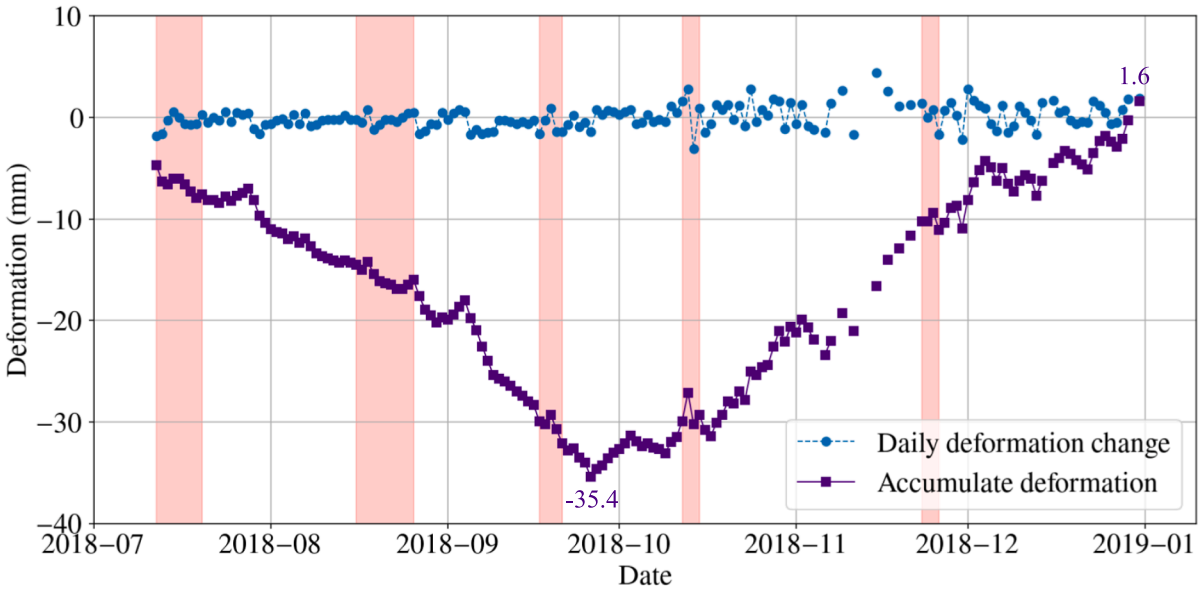

(c) D7-5(43.5m)

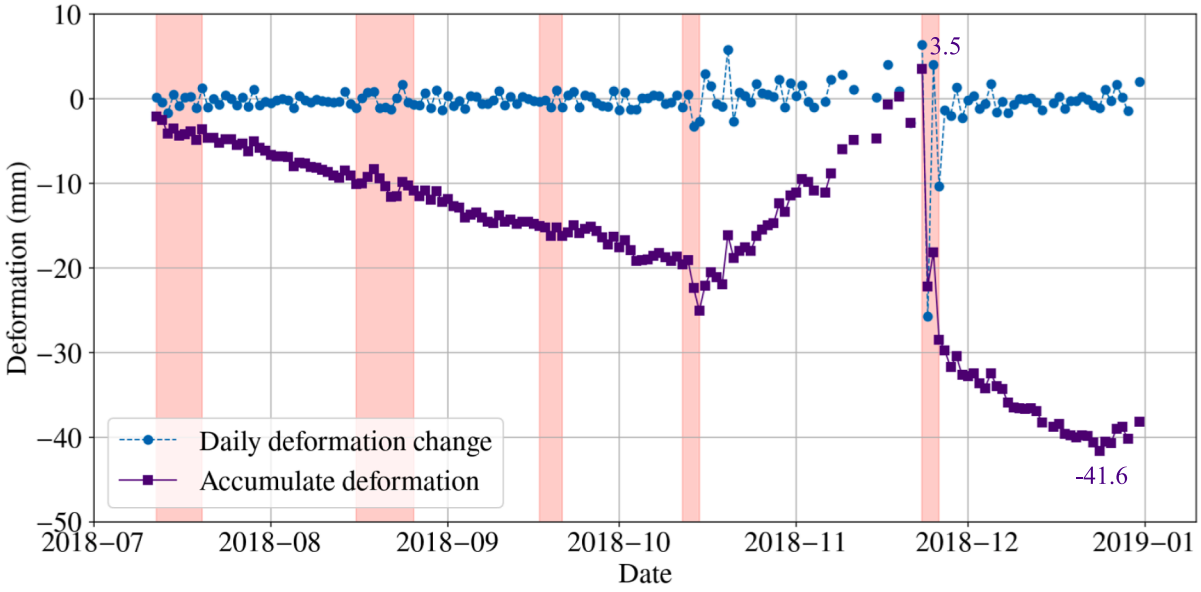

(d) D10-5(64m)

Fig. 13. (*continued*).

maximum heave of 120 mm, while the ground surface remains a subsidence mode except for a minor heave at 0–20 m range. Moreover, as depicted in Fig. 15(e), following the completion of the 5th culvert jacking, the pipe deformation ranges between 50 mm and 200 mm, whereas surface deformation fluctuates within a ± 20 mm range, indicating the magnitude of pipe deformation is significantly greater than that of surface.

3.3. Jacking force variations

The earth pressure measured within the front soil chamber, along with the jacking force, is presented in Fig. 16. At the initial stage of the first culvert jacking, the earth pressure is minimal, as the reinforced ground can maintain self-stability without the need for face support pressure. However, upon entering the natural ground (beyond 5 m), the earth pressure rises sharply, reaching a peak of 0.2 MPa at 7 m, before rapidly decreasing to 0.12 MPa at 10 m. This pronounced fluctuation in earth pressure within this section is likely attributable to suboptimal soil discharge control during the early phase of jacking. During the second culvert jacking, the earth pressure decreases from 0.13 MPa and eventually stabilizes at 0.075 MPa. Subsequently, at the commencement of the third culvert jacking, the pressure increases from 0.075 MPa to 0.11 MPa, a level that is maintained through the completion of the fourth culvert jacking. Notably, the fifth culvert jacking is characterized by more significant fluctuations in earth pressure, which then decline sharply as the shield passes through the reinforced ground outside the

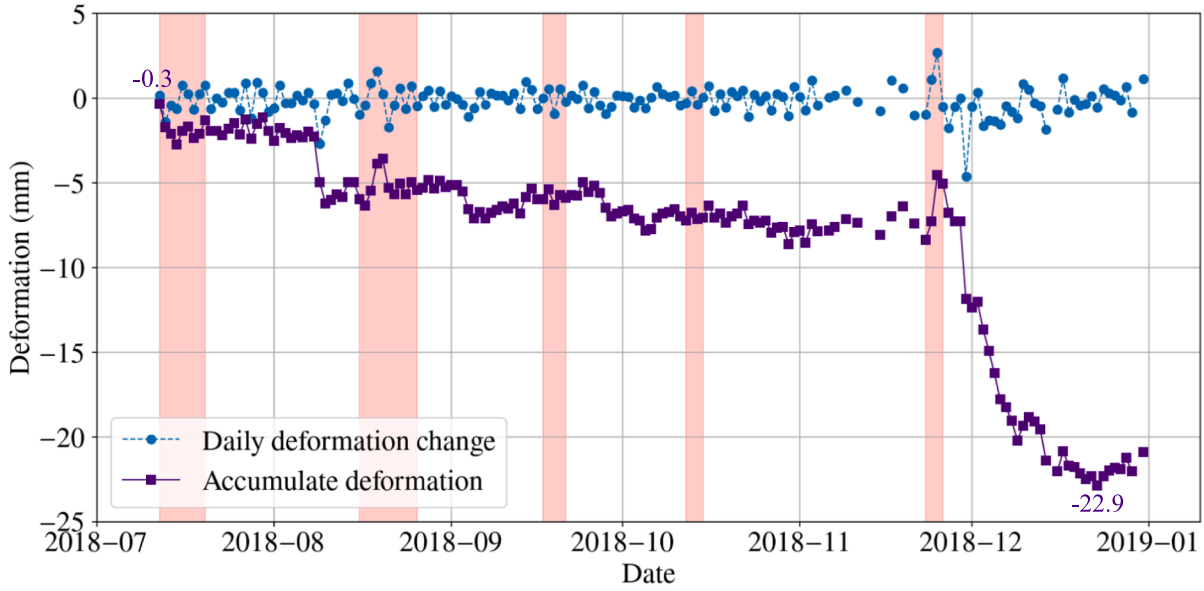

(e)D12-4(80m)

Fig. 13. (*continued*).

reception shaft and is ultimately received.

The jacking force exhibits a rapid increase to a peak value of 78 MN during the initial stage (0–5 m), followed by a sharp decrease between 5 and 10 m. Subsequently, it stabilizes within the range of 30 to 50 MN, with minor local fluctuations, up to a distance of 50 m. Beyond this point, the jacking force gradually increases, reaching a higher plateau and attaining a local maximum of 69 MN at 52 m. From 66 m to the reception end, it displays more pronounced fluctuations. Additionally, it is evident that at the commencement of each culvert jacking, there is a notable local increase in the jacking force, which then gradually decreases to a stable value. The friction force, calculated by subtracting the earth pressure force from the total jacking force, is also presented in Fig. 16. It can be observed that during the first culvert jacking, the friction force closely follows the trend of the jacking force, while significant fluctuations are evident during the jacking of the subsequent four culverts.

A comparison of the jacking force and earth pressure suggests that, when traversing the reinforced ground volume (outside the shafts), the friction force becomes the predominant factor. Over the long term, from the second to the fifth culvert jacking, the friction force exhibits an overall increasing trend, despite notable local fluctuations. In contrast, the earth pressure does not display a similar long-term increasing trend from the third to the fifth culvert jacking, indicating that earth pressure is primarily governed by the pressure balance at the tunnel face.

In culvert jacking tunnelling, the required jacking force is generally estimated prior to project implementation. For instance, the foundation design code in Shanghai (2019) offers a method for quantifying the forces:

$$F_S = \gamma_F N_F + \gamma_S N_S \tag{4}$$

$$N_F = \gamma h_0 \tan^2(45^\circ + \frac{\varphi}{2}) B_M H_M \tag{5}$$

$$N_S = [C_S(B + 2H) + \mu(G_k + \gamma hB)]L \tag{6}$$

In the formula,F_S is the estimated total jacking force (kN), γ_F is the itemized coefficient of shield face resistance (1.2 in this study), N_F is the standard value of shield face resistance (kN); γ_s is the itemized coefficient of culvert peripheral resistance(1.3 as proposed) and N_s standard value of total friction resistance (kN). h_0 is the depth of the centre point of the shield head (m); C_s is the average friction intensity between the culvert and pipe roof (kN/m2), which can be set as 5 as proposed; μ is the friction coefficient of the bottom of the box culvert, which can take 0.12; G_k is the standard value of culvert weight per unit length (kN/m); B and H is the width and height of the culvert, and h is the depth of culvert top; B_M and H_M are the width and height of the EPB shield, and L is the total length of the jacking. Considering the depth of the shield cutter head, the properties of the soil are taken as a weighted average, the natural weight of the soilγ = 17.1 kN/m^2, and the friction angleφ = 11.8°. In this project, h_0=10.99 m, h=7.58 m.B_M = 19.84 m, H_M=6.42 m, B=19.8 m, H=6.4 m.G_k = 1477kN/m. By substituting the above parameters into Eq. (4), the results are plotted in Fig. 16. Although the earth pressure at shield head is generally assumed passive earth pressure (P) (as demonstrated in Eqs. (5), the cases of at-rest (R) and active earth pressures (A) are also considered in the analysis, with the calculation results and monitoring results displayed in Fig. 17.

As the calculations do not explicitly consider the presence of the reinforced soil zone during the initial stage of jacking, it underestimates the required jacking force for the first culvert. It is evident that, following the first culvert, estimates based on passive earth pressure assumptions generally overestimate the total jacking force, with the exception of certain segments, such as between 12.5 m and 25 m, where a good correspondence with measured values is observed. Excluding the results within the reinforced zone, the estimates derived from passive earth pressure calculations yield relatively conservative values, effectively encompassing the peak forces observed at the onset of each culvert jacking. This characteristic renders the passive earth pressure approach more suitable for engineering design purposes. In contrast, estimates based on at-rest and active earth pressures tend to underestimate the force values partially, although they correspond well with the overall increasing trend of the jacking force. These findings suggest that, in actual jacking operations, the soil at the tunnel face may tend to exhibit complex earth pressure conditions, a behaviour that is closely associated with soil discharge control in EPB shield tunnelling.

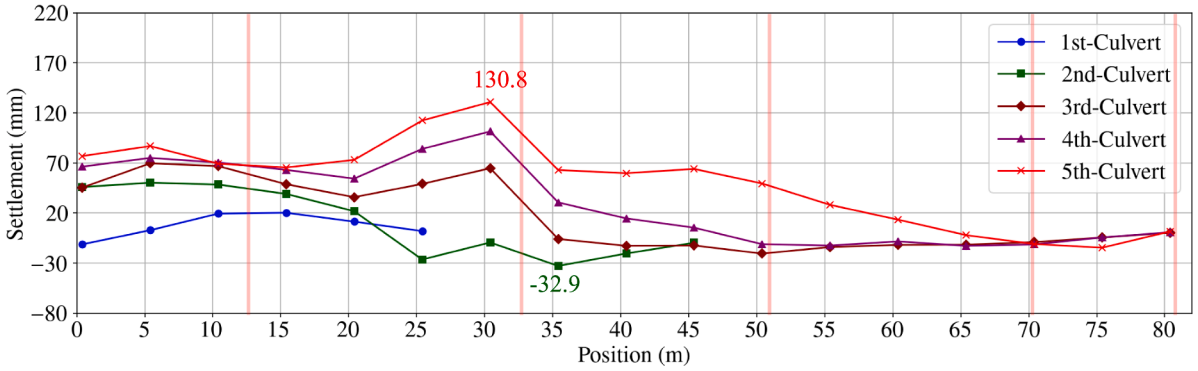

(a) S5

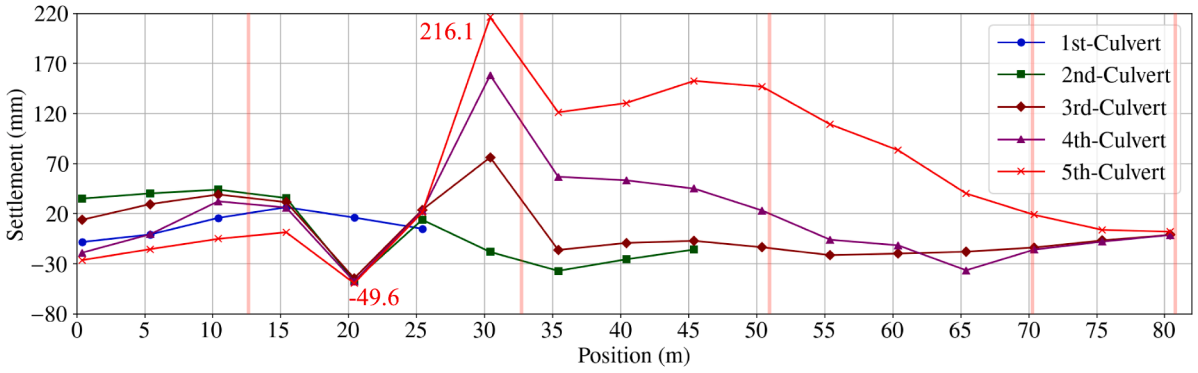

(b) S11

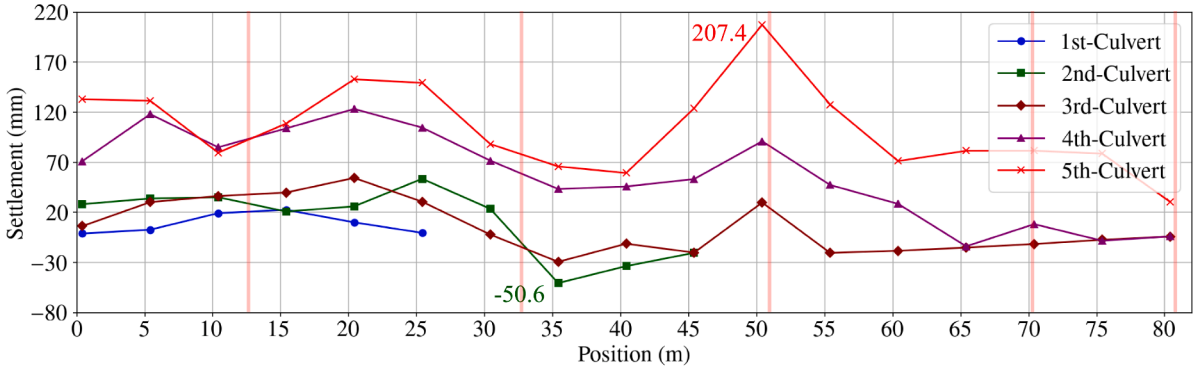

(c) S14

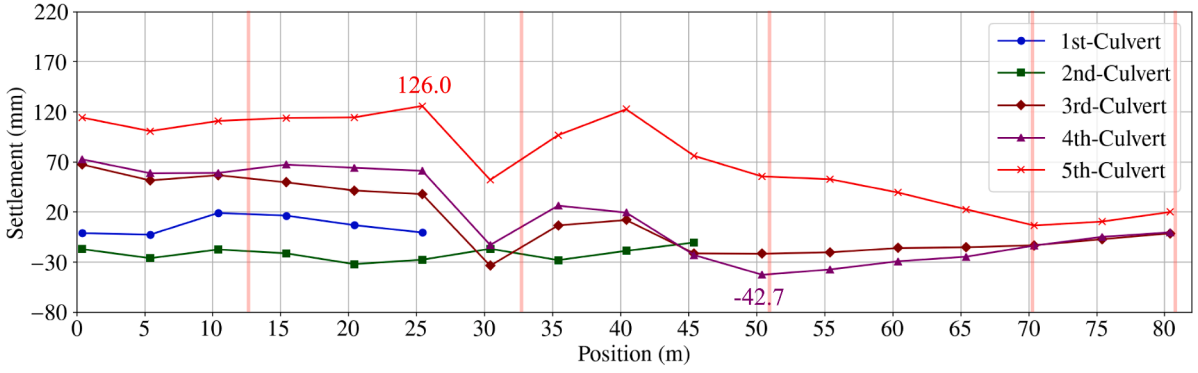

(d) S20

Fig. 14. Accumulated deformation of pipe-roof after each culvert jacking.

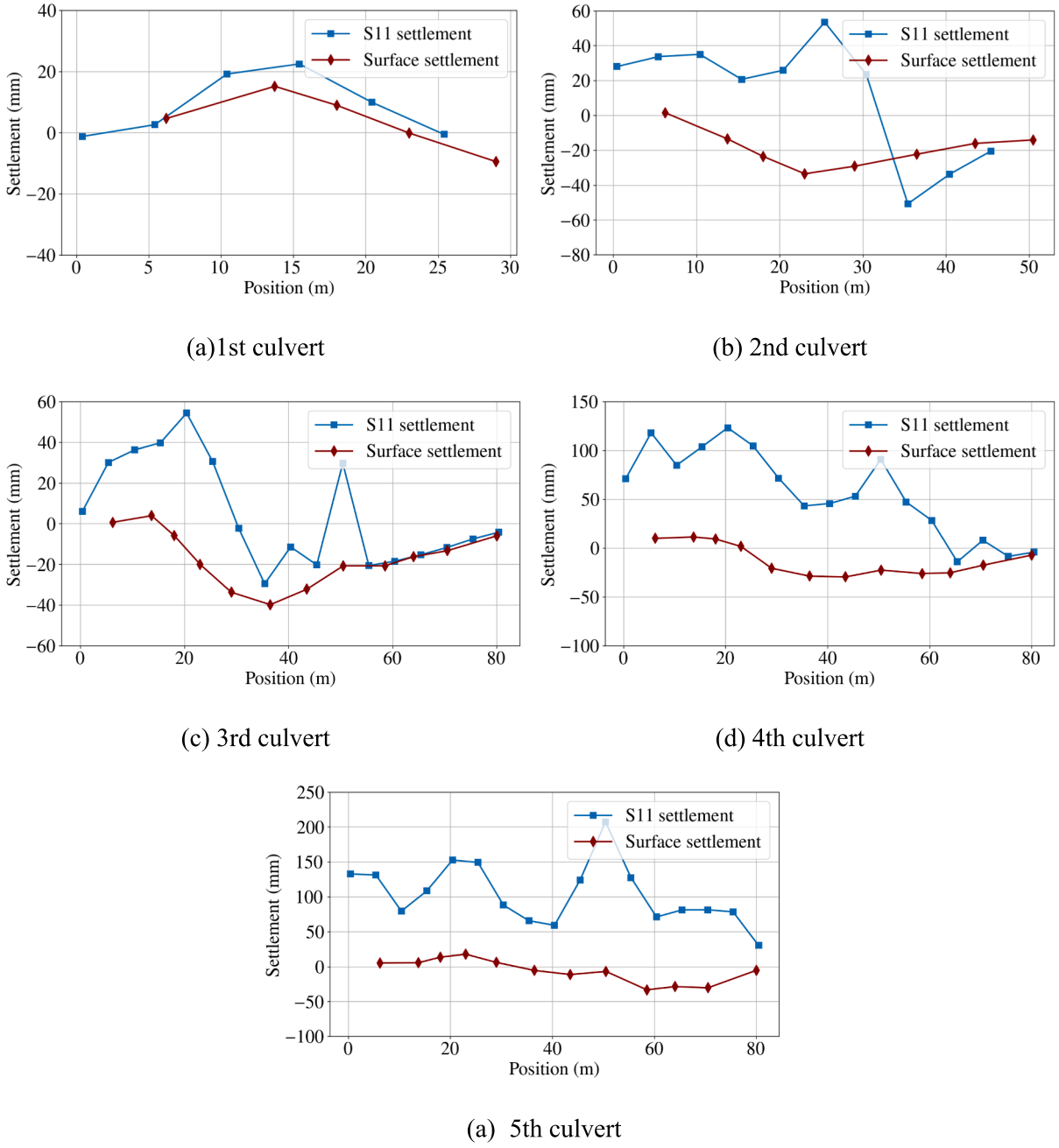

Fig. 15. Comparison of accumulated deformation of pipe S11 and surface settlement after each culvert jacking.

4. Numerical simulation

4.1. Numerical model

The demonstrated monitoring data in above sections reveal that characteristics of ground deformations is closely related to the construction operation, such as the setting of grouting and face pressures in culvert jacking process, and therefore it is meaningful to investigate their corresponding effects on the ground deformation behaviours throughout culvert jacking. This section conducts a finite element numerical simulation using software PLAXIS 3D to specifically study the impacts of lubrication grouting and face support pressures on ground settlements. Given the symmetrical nature of the soil domain and structure, the full model dimensions (shown in Fig. 18) are determined to be 30 m × 86 m × 30.5 m (width × length × height), and tunnel excavation area has dimensions of 9.9 m × 86 m × 6.4 m. The coordinate of the surface in the z-axis is set to + 4.5 m, with a ground water head of + 1.25 m.

Table 4 presents the primary physical and mechanical properties of the soil strata for this numerical model. The Poisson's ratio for all soil layers is set to 0.2. In the FEM model, the hardening soil model is used to simulate the behaviours of soil in tunnelling process. The top and side boundaries of the soil domain are defined as hydraulically permeable, while the bottom boundary is impermeable. Two soil blocks, each 13 m long, 3 m wide, and 16.5 m high, are set on both ends of the culvert tunnel (just outside the launch and reception shafts) improved by soil mixing using high-pressure rotatory jetting, to mitigate settlement and water inrush risks when the EPB shield is launched and received. The reinforced soils are modelled using an elastic model and a stiffness of 4.4 × 10^4 MPa. Since the thin hollow pipe tubes are filled with concrete before culvert jacking starts, here the pipe is modelled as concrete with the same stiffness as the improved soil. Grouting pressure and front face

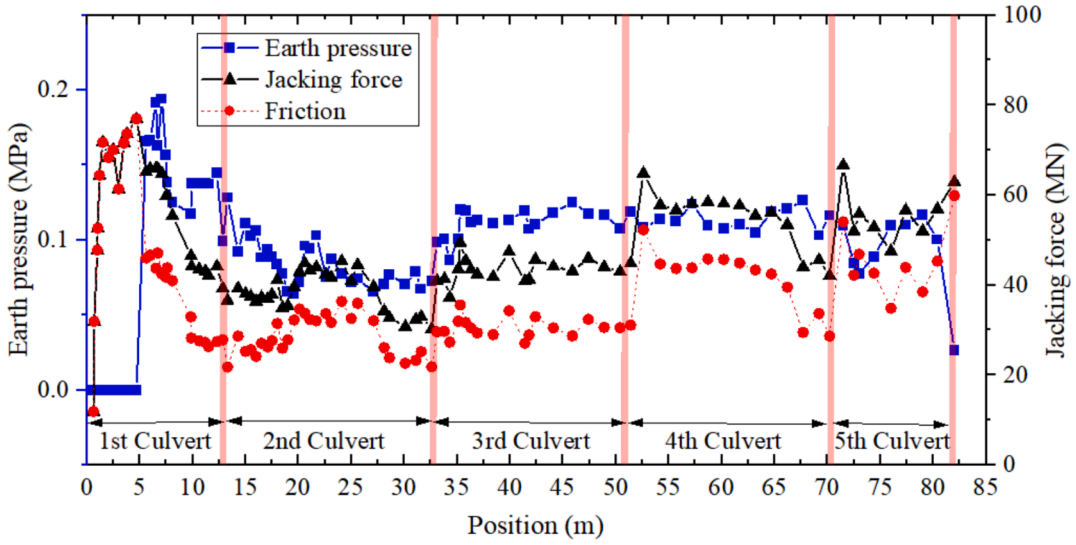

Fig. 16. Variation of front earth pressure and total jacking force.

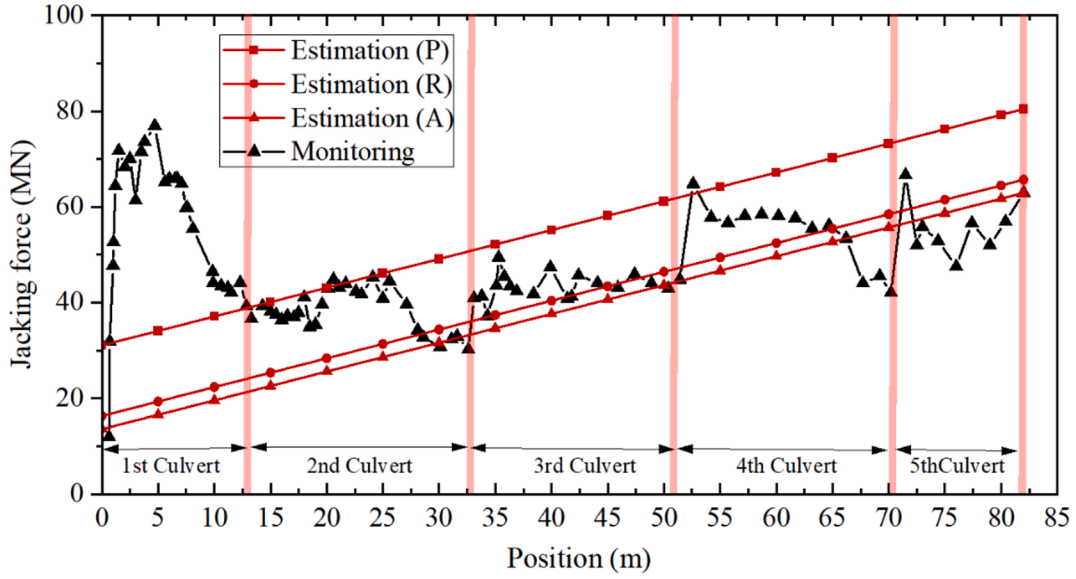

Fig. 17. The comparison of estimated jacking force with monitoring results.

pressure are simulated by applying normal surface pressures in PLAXIS 3D (see Fig. 18).

4.2. *Impacts of grouting pressure*

In the finite element analysis, the impact of grouting pressure on ground surface settlement is firstly investigated, and the second culvert jacking process is simulated to analyse the surface settlement under different grouting pressures applied. The jacking process (length of 18.8 m) lasts for nine days, and accordingly a total of nine construction steps are set in PLAXIS 3D simulation, with each step corresponding to one day's jacking work in the actual construction process. In the simulation, the front face pressure is set a constant 75 kPa and the grouting pressure is set 100 kPa for the first eight steps, but at the final ninth step three different scenarios with variable grouting pressure (0 kPa, 50 kPa, and 100 kPa) are applied at the excavation face of the second culvert to represent low, medium, and high grouting pressure levels, while the corresponding ground surface settlements are obtained for analysis.

Fig. 19 presents the vertical ground settlement above the second culvert, under grouting pressures of 0 kPa, 50 kPa, and 100 kPa, respectively. As shown in Fig. 19(a), when the grouting pressure is set to 0 kPa, the maximum surface settlement reaches −26 mm along the length of the second culvert. When the grouting pressure is increased to 50 kPa and 100 kPa, the maximum surface settlement decreases to −20 mm and −12 mm, corresponding to reductions of 23 % and 53.8 %, respectively, as illustrated in Fig. 19(b) and (c). These results indicate that increasing the grouting pressure significantly contributes to the reduction of ground settlement during culvert jacking. Fig. 20 presents the settlements recorded at nine surface monitoring points at the final stage of construction, with the excavation face positioned at 0 m. The results indicate that surface settlement increases as the monitoring points approach the excavation face. Specifically, when the grouting pressure is 0 kPa, surface settlement rises from −13 mm to −25.5 mm near the excavation face. A similar trend is observed at a grouting pressure of 50 kPa, with settlement increasing from −10.5 mm to −19 mm, and at 100 kPa, from −8 mm to −12.8 mm. Overall, these findings demonstrate that effective control of grouting pressure is crucial for mitigating ground disturbance during construction.

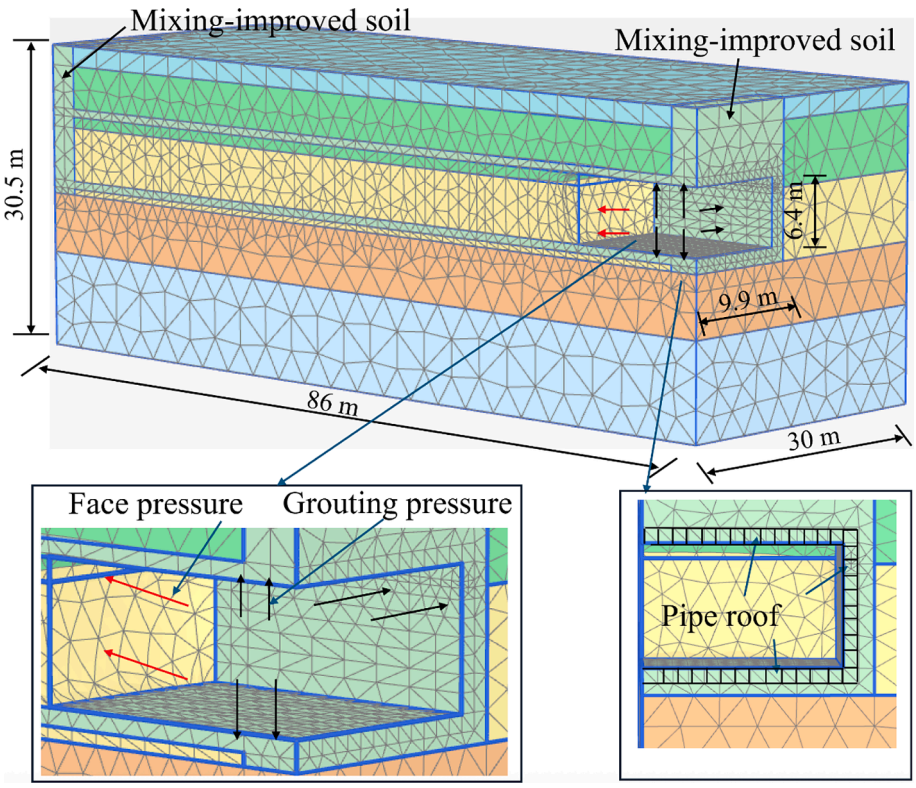

Fig. 18. Three-dimensional numerical model of culvert jacking tunnelling.

Table 4
Geological parameters of ground strata.

Soil type	Thickness (m)	Unit weight (kN/m^3)	Friction angle φ(°)	Cohesion (kPa)	Compression modulus E_s (MPa)
Silty clay-1	2.00	18.5	19	19.0	4.46
Muddy silty clay	6.20	17.5	18.0	12.0	3.09
Muddy clay	6.80	16.8	11.5	11.0	2.20
Silty clay-2	6.00	17.9	19.0	14.0	3.79
Silty sand	9.50	18.5	31.0	5.00	9.43

4.3. Impacts of face pressure

During culvert jacking tunnelling, front face pressure is another critical factor affecting surface settlement, alongside grouting pressure. During the simulation, the grouting pressure is kept constant at 100 kPa, while the face pressures for the first eight steps are determined based on field EPB earth pressure monitoring (from the 1st to the 8th, 92 kPa,111 kPa, 100 kPa, 76 kPa, 86 kPa, 78 kPa, 70 kPa, 71 kPa). At the final construction step, three different face pressures (25 kPa, 75 kPa, and 125 kPa) are applied, representing low, medium, and high face pressure levels. The resulting ground deformations are then analysed.

Fig. 21 depicts the vertical ground deformations under face support pressures of 25 kPa, 75 kPa, and 125 kPa, respectively. As shown in Fig. 21(a), when the face pressure is set to 25 kPa, the maximum surface settlement reaches −24 mm. Increasing the face pressure to 75 kPa and 125 kPa reduces the maximum settlement to −13 mm and −12 mm, corresponding to decreases of 45.8 % and 50 %, respectively, as depicted in Fig. 21(b) and 21(c). These results indicate that increasing the face pressure is effective in reducing ground settlement; however, excessively high face pressures do not yield significant additional benefits. Furthermore, Fig. 22 presents the surface settlements at nine monitoring points along the jacking length of the second culvert under different face pressures. It can be observed that increasing the face pressure from 25 kPa to 75 kPa substantially mitigates settlement, with the maximum value decreasing from –23.4 mm to −12.8 mm. However, a further increase in face pressure from 75 kPa to 125 kPa only reduces the maximum settlement to −12 mm, indicating a marginal effect on settlement mitigation. These findings suggest that applying a face pressure above 75 kPa does not significantly enhance settlement control during culvert jacking.

4.4. Discussion and limitations

Based on the preceding analysis, it is instructive to compare the effects of grouting pressure and face pressure on surface settlement, as is commonly done in shield tunnelling studies (Zhang et al., 2018). When the grouting pressure is increased from 0 to 50 kPa, the maximum surface settlement decreases from −26 mm to −20 mm, representing a reduction of 23.1 %. In contrast, increasing the face pressure from 25 to 75 kPa results in a decrease in maximum surface settlement from −24 mm to −13 mm, corresponding to a reduction of 45.8 %. This indicates that, within this range, increasing face pressure (when below 75 kPa) is more effective than increasing grouting pressure in mitigating settlement. However, further increasing the grouting pressure to 100 kPa reduces the maximum settlement from −20 mm to −12 mm, amounting to a 40 % reduction. In comparison, increasing the face pressure from 75 kPa to 125 kPa only decreases the maximum settlement from −13 mm to −12 mm, a reduction of 7.7 %, indicating a diminished sensitivity of surface settlement to face pressure at higher values. These findings suggest that while increasing face pressure is initially more effective for settlement control, the effectiveness plateaus at higher pressures, whereas increasing grouting pressure continues to yield substantial

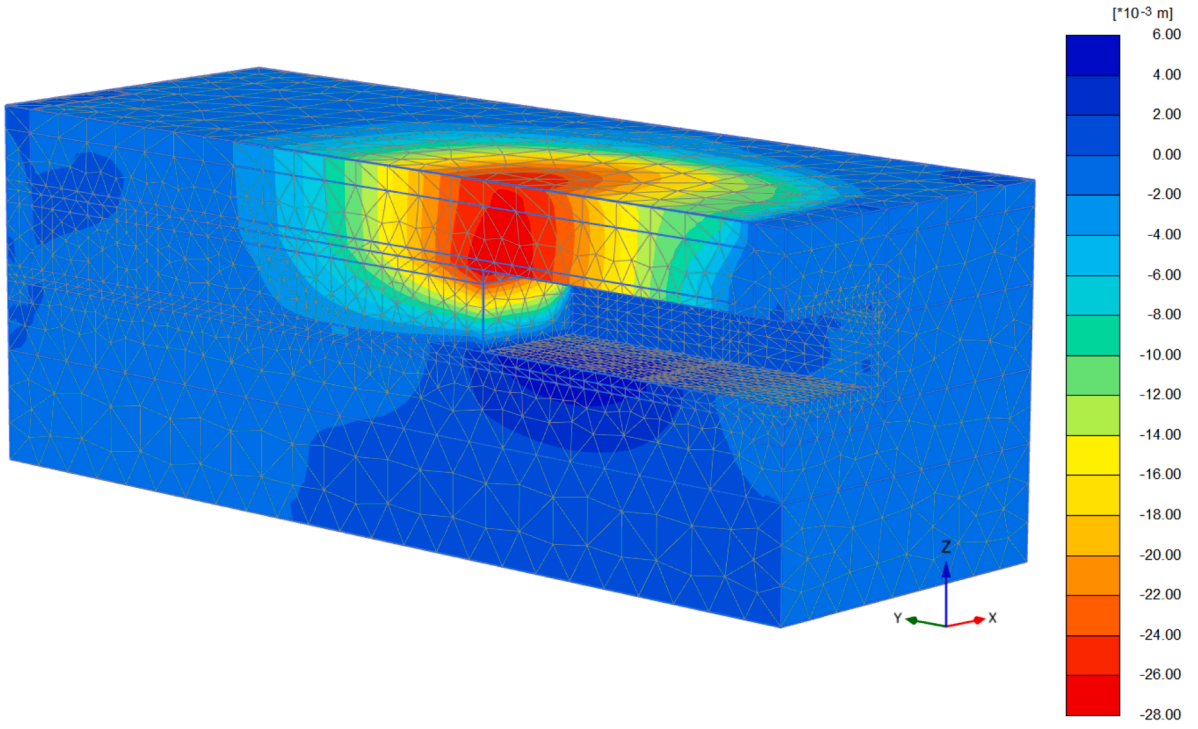

(a) Grouting pressure of 0 kPa

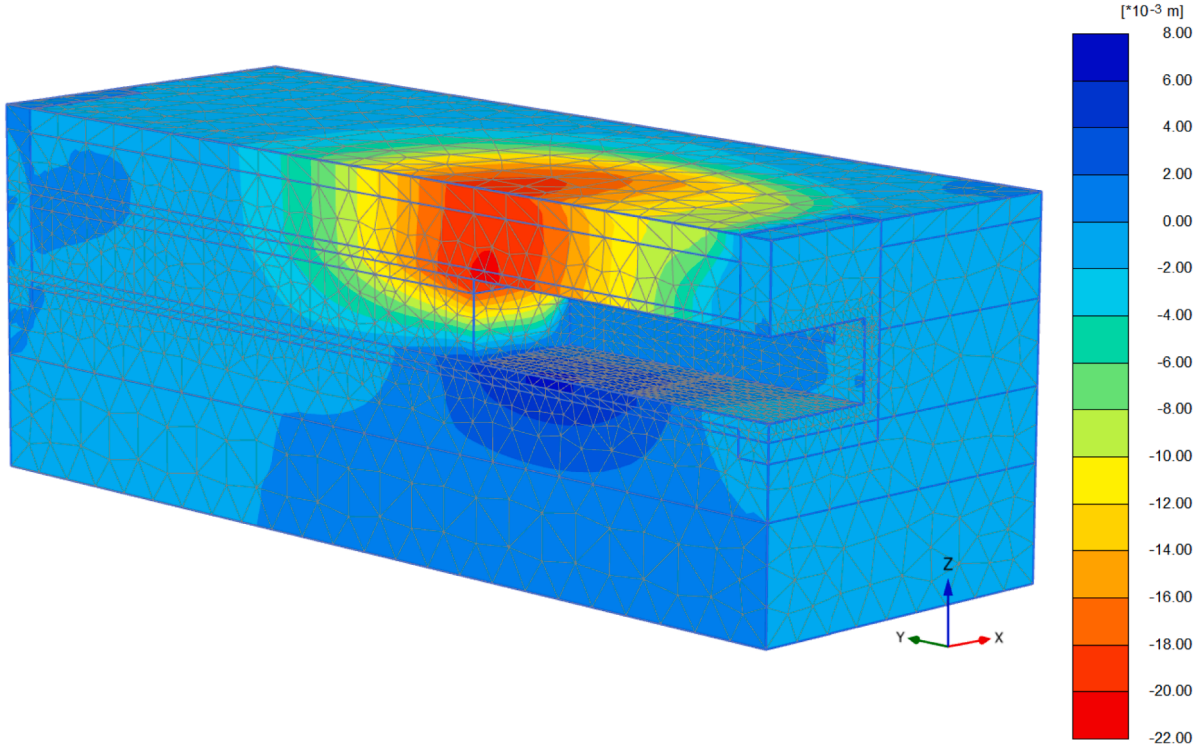

(b) Grouting pressure of 50 kPa

Fig. 19. Ground deformations of the second culvert jacking at different grouting pressures.

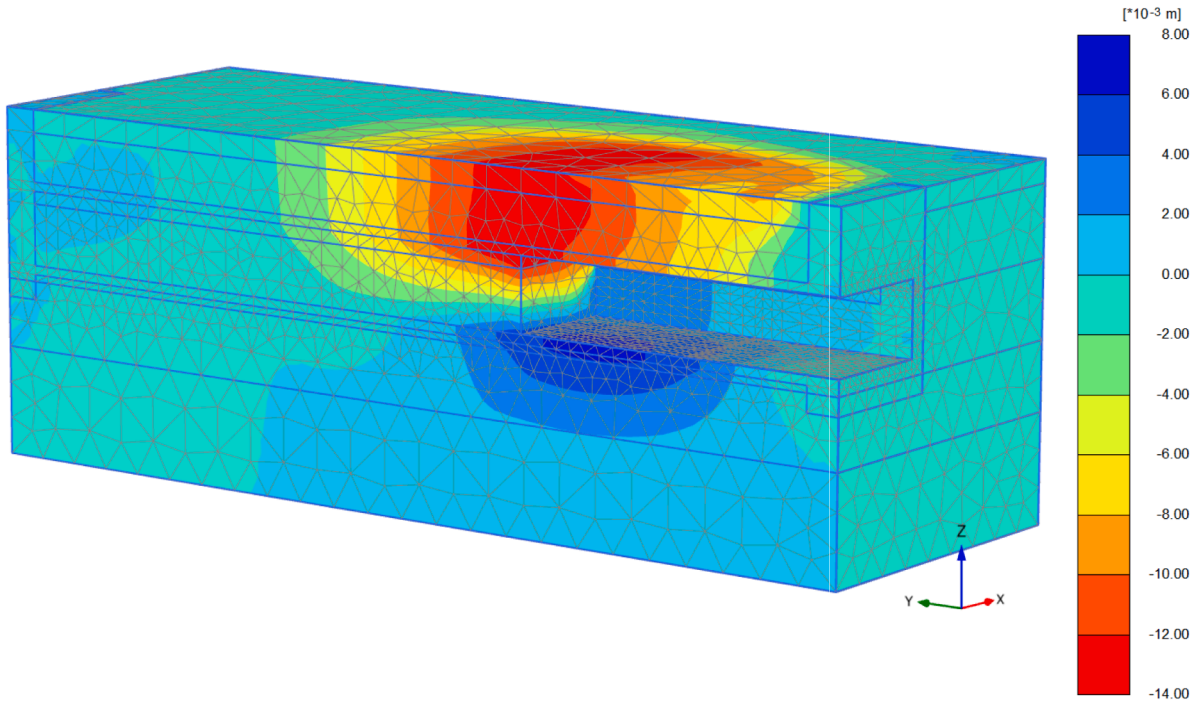

(c) Grouting pressure of 100 kPa

Fig. 19. (*continued*).

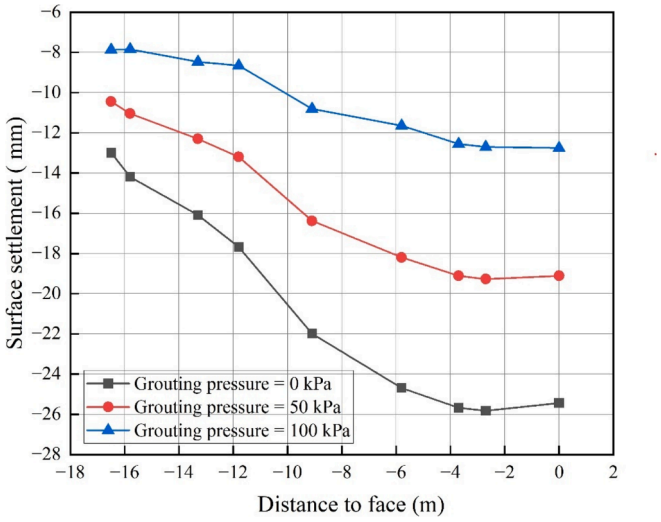

Fig. 20. Surface settlement variations with different grouting pressures.

reductions in settlement. Therefore, in PPM culvert jacking, increasing both grouting and face pressures is effective in mitigating surface settlement. Simulation results suggest that maintaining a grouting pressure of 100 kPa and a face pressure of 75 kPa can generally limit the maximum surface settlement to approximately 13 mm. Furthermore, increasing the face pressure beyond 75 kPa does not provide significant additional benefits for settlement control.

Another important aspect is the comparison between numerical simulation results and monitoring data. It should be noted that accurately simulating the culvert jacking process with a pipe roof presents several technical challenges in this study. These include the precise spatial distribution and temporal variation of grouting pressure, the vertical distribution and fluctuation of face pressure on the excavation face, and the influence of pipe installation errors, which result in complex contact conditions between the culvert and the pipe. Consequently, this study does not attempt to achieve an exact match between simulation and monitoring data. For instance, as shown in Fig. 23, a reasonable agreement between monitored settlements and simulation results can be obtained by adopting a potential combination of instantaneous grouting and face pressures as specified in Table 5. However, in the absence of measured pressure data, it is difficult to conduct precise real-time simulations, and therefore, such analyses are not pursued in this study.

Furthermore, there exist limitations in this numerical simulation. Firstly, due to the lack of spatial and temporal distribution information of the grouting pressure along the outer tunnel circumference, this simulation fails to match monitoring data. Secondly, the inter-pipe connection, namely the special socket-plug joint in this project, with its mechanical behaviours is not considered, while the pipe roof is modelled using a concrete plate for simplicity. Note that the inter-pipe joint shows relatively higher flexibility and significant deformation tends to occur under impacts of ununiform grouting pressure. In addition, the influence of pipe installation deviations on the ground deformations is not considered due to a difficulty in charactering the interface contact and a lack of detailed pipe monitoring data. To address the aforementioned limitations, it is recommended to implement more precise monitoring of the spatial and temporal distribution of grouting pressure along the entire tunnel length, for example, by employing distributed sensing systems (Zhang and Broere, 2023; Zhang et al., 2024). Such detailed pressure data would facilitate a better understanding of ground response under various grouting modes. Furthermore, to investigate the mechanical behaviour of socket-plug pipe connections, laboratory load tests are advised to characterise the joints' shear and tensile properties, which would enable the development of more accurate numerical models. Additionally, to enhance ground disturbance control, the exploration of advanced algorithms is recommended. These algorithms should relate construction parameters (such

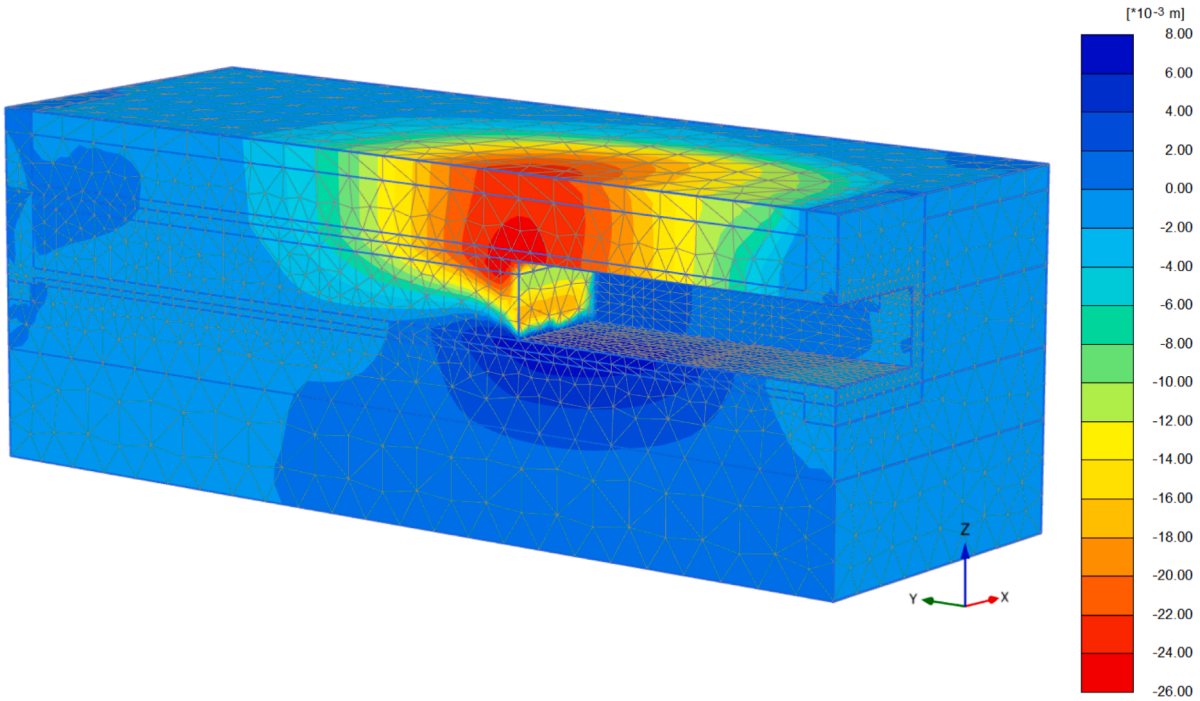

(a) Face pressure of 25 kPa

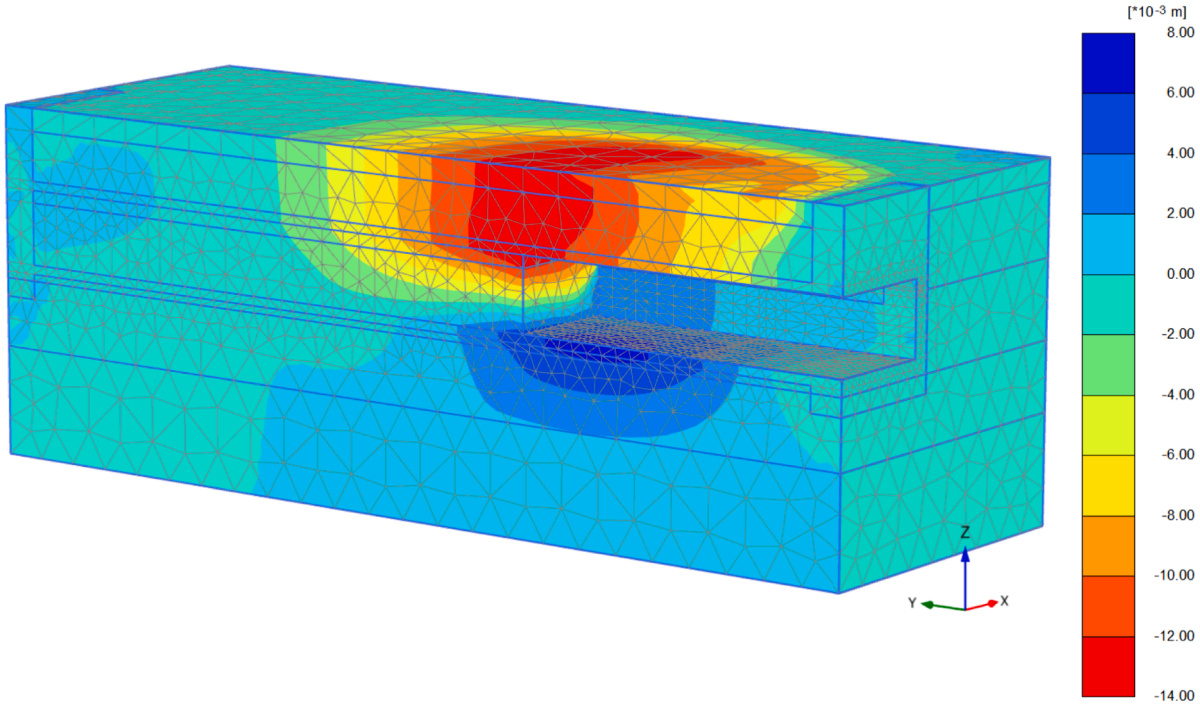

(b) Face pressure of 75 kPa

Fig. 21. Ground deformations of the second culvert jacking at different face pressures.

as pressure and soil discharge rate) to real-time ground response, thereby enabling valuable real-time evaluation and feedback during culvert jacking tunnelling operations.

5. Conclusion

This study examines the ground deformation characteristics associated with EPB culvert jacking tunnelling combining with the pipe-roof

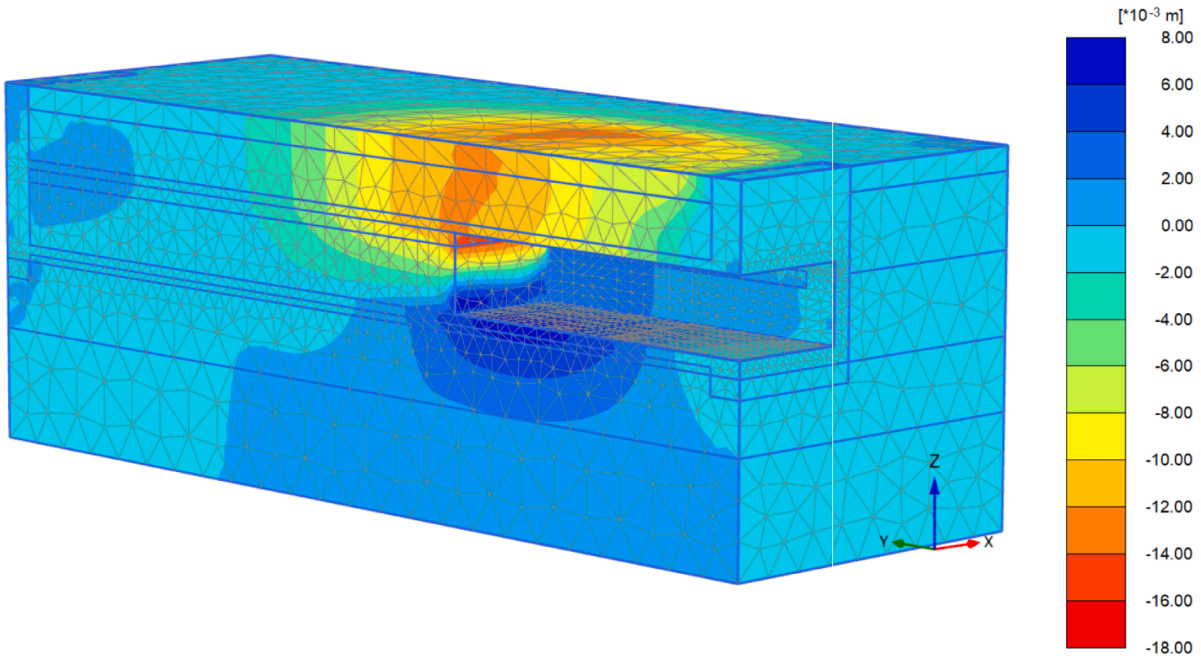

(c) Face pressure of 125 kPa

Fig. 21. (*continued*).

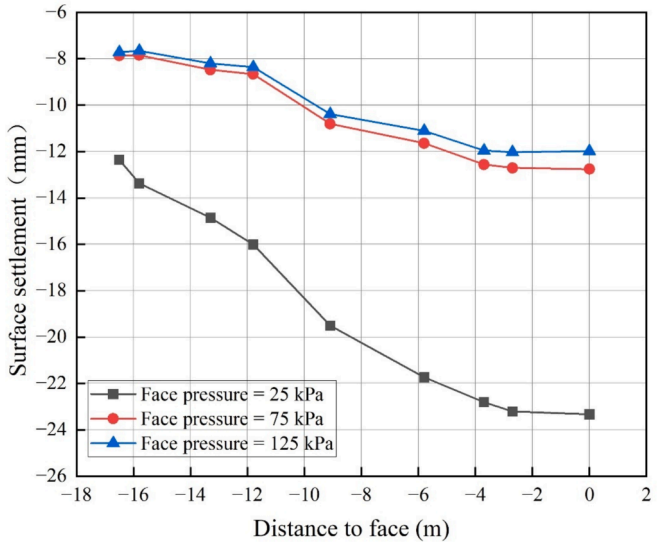

Fig. 22. Surface settlement variations with different face pressures.

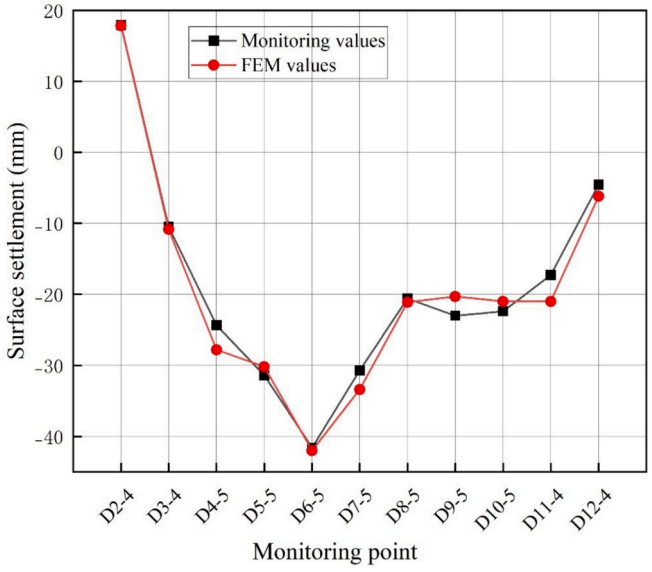

Fig. 23. Surface settlement at monitoring points versus finite element modeling (FEM) values.

preconstruction method (PPM). The investigation is based on the largest (to date) case underpass tunnel project featuring a cross-section measuring 19.8 m in width and 6.4 m in height. The research involves a detailed analysis of the deformation time-history of both the ground strata and the pipe roof, supported by extensive monitoring throughout the culvert jacking process. Additionally, a three-dimensional numerical simulation is conducted to further understand the deformation evolution and control. The main conclusions can be drawn as follows:

(1) Longitudinally, the jacking of individual culvert segments typically results in surface settlement along the tunnel axis, with the maximum settlement change reaching 40 mm during the jacking of the third culvert. The pressures from lubrication grouting have a significant impact on ground deformation, particularly along the excavated length behind the front face.

(2) Transversely, the profile of the tunnel's front face generally displays a V-shaped settlement trough, with the greatest deformation occurring at the centre of the tunnel cross-section. However, the transverse settlement profile varies significantly due to the continuous jacking operation and is influenced by both ground loss and grouting pressures.

(3) During the culvert jacking process, the pipe roof exhibits a substantially greater scale of vertical deformation compared to the ground surface. This underscores the sensitivity of the pipe roof

Table 5
Grouting pressure at monitoring points when tunnel face progresses.

Monitoring point	D2-4	D3-4	D4-5	D5-5	D6-5	D7-5	D8-5	D9-5	D10-5	D11-4	D12-4
Grouting pressure (kPa)	800	100	100	180	260	320	350	320	280	450	800
Face pressure (kPa)	92	66	72	75	115	118	113	113	118	110	350

to disturbances induced by culvert jacking, while the surface deformation is mitigated by the presence of the pipe roof.

(4) Jacking force estimates based on passive earth pressure calculations, although provide relatively conservative values, effectively covers the peak forces observed and hence appliable for engineering design.

(5) The three-dimensional numerical simulation indicates that while both lubrication grouting pressures and front face pressures influence ground surface deformations, while increasing face pressure is initially more effective for settlement control, the effectiveness plateaus at higher pressures, whereas increasing grouting pressure continues to yield substantial reductions in settlement. This suggests that controlling ground disturbance necessitate a proper managing of lubrication grouting and face pressures during culvert jacking.

CRediT authorship contribution statement

Xuehui Zhang: Writing – review & editing, Writing – original draft, Supervision, Resources, Methodology, Conceptualization. **Jiantuan Qin:** Writing – original draft, Software, Investigation, Data curation. **Xiao Zhang:** Writing – review & editing, Resources, Conceptualization. **Jiarui Zhang:** Writing – review & editing, Writing – original draft, Visualization, Methodology, Formal analysis, Data curation. **Xi Jiang:** Writing – review & editing.

Declaration of competing interest

The authors declare that they have no known competing financial interests or personal relationships that could have appeared to influence the work reported in this paper.

Data availability

the data supporting the findings of this study are available within the article.

References

Bai, Y., Jiang, X., Diaz, D., Zhang, X., TBMs, Zhang, Z., 2018. Capabilities, Limitations and Challenges. International Conference: Tunnelling and Underground Construction. Springer Singapore, Singapore, pp. 528–535.

Chen, S.-L., Chang, S.-W., Qiu, Z.-Y., Tang, C.-W., Zhang, X.-L., Chen, Y., 2023. Numerical model for rectangular pedestrian underpass excavations with pipe-roof preconstruction method: A case study. Appl. Sci. 13 (10), 5952. https://doi.org/10.3390/app13105952.

Chen, X., Ma, B., Najafi, M., Zhang, P., L,, 2021. Rectangular Box Jacking Project: A Case Study. Underground Space 6 (2), 101125. https://doi.org/10.1016/j.undsp.2019.08.003.

Foundation design code, 2019. Shanghai Municipal Commission of Housing and Urban-rural Development, DGJ08-11-2018 (in Chinese).

Hao, Z., Zhang, H., Zhang, G., Xiong, W., Wang, L., 2022. The prediction of ground settlement of a box culvert jacked under the action of an ultra-shallow buried pipe curtain. Arabian Journal for Science and Engineering 47 (10), 12423–12438.

He, J., Liao, S., Tan, Y., Liu, M., 2022. Field measurement on the interaction between socketed pipes during pipe-roof jacking in soft ground and corresponding surface settlement. Tunnell. Underground Space Technol. 130, 104769.

Jia, P., Zhao, W., Khoshghalb, A., Ni, P., Jiang, B., Chen, Y., Li, S., 2020. A new model to predict ground surface settlement induced by jacked pipes with flanges. Tunn. Undergr. Space Technol. 98, 103330.

Jiang, X., Zhang, X., Wang, S., Bai, Y., Huang, B., 2022. Case Study of the Largest Concrete Earth Pressure Balance Pipe-Jacking Project in the World. Transportation Research Record: Journal of the Transportation Research Board. 2676, 92–105.

Jiang, X., Zhang, X., Zhang, X., Long, L., Bai, Y., Huang, B., 2024. Advancing Shallow Tunnel Construction in Soft Ground: The Pipe-Umbrella Box Jacking Method. Transp. Res. Rec. 03611981231225430.

Jiang, X., Zhu, H., Yan, Z., Zhang, F., Ye, F., Li, P., Zhang, X., Dai, Z., Bai, Y., Huang, B., 2023. A state-of-art review on development and progress of backfill grouting materials for shield tunneling. Dev. Built Environ. 16, 100250.

Kim, J., Kim, J., Rehman, H., Yoo, H., 2020. Ground Stability Analysis in Non-Open-Cut Tunneling Method Using Small-Diameter Steel Pipe Piles. Appl. Sci. 10 (19), 6906. https://doi.org/10.3390/app10196906.

Li, P., Liu, X., Jiang, X., Zhang, X., Wu, J., 2024. Investigation of the First Quasi-Rectangular Metro Tunnel Constructed by the 0−θ Method. Front. Struct. Civ. Eng. 17 (11), 1707–1722.doi. https://doi.org/10.1007/s11709-023-0991-9#citeas.

Lu, B., Jia, P., Zhao, W., Zheng, Q., Du, X., Tang, X., 2023. Longitudinal mechanical force mechanism and structural design of steel tube slab structures. Tunn. Undergr. Space Technol. 132, 104883.

Niu, J., 2019. Application of Micro-Disturbance Propulsion Construction Technology for Large Cross-Section Box Culvert Tunnel. Construction 39 (11), 1905. https://doi.org/10.3973/j.issn.2096-4498.2019.11.020.

Peck RB (1969) Deep excavation and tunnelling in soft grounds. In: 7th international conference on soil mechanics and foundation engineering, Mexico City, State of the Art Volume, pp 225–290.

Powderham, A., Howe, C., Caserta, A., Allenby, D., Ropkins, J., 2004. Boston's Massive Jacked Tunnels Set New Benchmark. Proc. Inst. Civ. Eng. Civ. Eng. 157 (2), 70–78. https://doi.org/10.1680/CIEN.2004.157.2.70.

Prakoso, W.A., Sabbah, A.B., 2016. Effect of nose blade angle on face stability of jacked box tunnelling. Jurnal Teknologi 78 (8–6), 9–14. https://doi.org/10.11113/jt.v78.9633.

Pritchard, M., T. Kucki, J. D. Boer. 2011. The design and construction of Cliffsend Underpass. In Proc., 6th Int. Conf. on Space Structures, 93–96. Johor, Malaysia: Jurnal Teknologi.

Tang, Z., Wang, H., Sun, D., Zhang, X., 2022. Surface displacement during pipe roof construction of pipe-jacking group with large section. Rock Soil Mech. 43, 1933–1941.

Wang, H., Qin, W.M., Jiao, Y.Y., 2013. Stability Assessment for Highway with Large-Span Box Culvert Jacking Underneath: A Case Study. Canadian Geotechnical Journal 50 (6), 585–594. https://doi.org/10.1139/cgj-2012-0334.

Wang, L., Chen, X., Su, D., Liu, S., Liu, X., Jiang, S., Yang, W., 2023. Mechanical performance of a prefabricated subway station structure constructed by twin closely-spaced rectangular pipe-jacking boxes. Tunnelling and Underground Space Technology 135, 105062.

Wang, Z., Hu, Z., Lai, J., Wang, H., Wang, K., Zan, W., 2019. Settlement Characteristics of Jacked Box Tunneling Underneath a Highway Embankment. J. Perform. Constr. Facil 33 (2), 04019005. https://doi.org/10.1061/(ASCE)CF.1943.

Xiao, S., Xia, C., Li, X., Zhu, H., Shen, G., Ge, J., 2005. Experimental study on coefficient of friction between a box culvert and mixture composed of thixotropic slurry and clay or steel pipe during culvert being pushed by pipe-roof. Chin. J. Rock Mech. Eng. 24 (15), 2746–2750 in Chinese.

Xie, X., Zhao, M., Shahrour, I., 2019. Face Stability Model for Rectangular Large Excavations Reinforced by Pipe Roof-ing. Tunn. Undergr. Space Technol. 94, 103132. https://doi.org/10.1016/j.tust.2019.103132.

Yang, H., Rong, L., Xu, H., 2016. Application of Drag Reduction Technology to Extra-Large Sectional Rectangular Pipe Jacking: Case Study of Tunnel Crossing Underneath Zhongzhou Road in Zhengzhou. Tunnel Construction 36 (4), 458–464. https://doi.org/10.3973/j/issn.1672-741X.2016.04.014.

Yang, S., Wang, M., Du, J., Guo, Y., Gen, Y., 2020. Influence of construction sequence of pipe jacking by pipe-roof pre-construction method on ground surface settlement. Journal of Zhejiang University (Engineering Science) 9 (54).

Yang, S., Wang, M., Du, J., Guo, Y., Geng, Y., Li, T., 2020. Research of jacking force of densely arranged pipe jacks process in pipe-roof pre-construction method. Tunn. Undergr. Space Technol. 97, 103277.

Yang, Y.F., Liao, S.M., Liu, M.B., Wu, D.P., Pan, W.Q., Li, H., 2022. A new construction method for metro stations in dense urban areas in Shanghai soft ground: Open-cut shafts combined with quasi-rectangular jacking boxes. Tunn. Undergr. Space Technol. 125, 104530.

Zhang, P., Ma, B.S., Zeng, C., Xie, H.M., Li, X., Wang, D.W., 2016. Key techniques for the largest curved pipe jacking roof to date: A case study of Gongbei tunnel. Tunn. Undergr. Space Technol. 59, 134–145. https://doi.org/10.1016/j.tust.2016.07.001.

Zhang, Y., Liao, S., Liu, M., Wang, H., Wu, D., 2022. Construction method and load characteristics of rectangular jacking box with central partition wall. Tunn. Undergr. Space Technol. 127, 105591. https://doi.org/10.1016/j.tust.2022.105591.

Zhang, X., Broere, W., 2023. Design of a distributed optical fiber sensor system for measuring immersed tunnel joint deformations. Tunn. Undergr. Space Technol. 131, 104770. https://doi.org/10.1016/j.tust.2022.104770.

Zhang, X., Zhu, H., Jiang, X., Broere, W., 2024. Designing a Distributed Sensing Network for Structural Health Monitoring of Concrete Tunnels: a Case Study. Struct. Control Health Monit. 2024 (1), 6087901. https://doi.org/10.1155/2024/6087901.

Zhang, X., Chen, J., Bai Y., Chen A., Huang D., 2024. Ground surface deformation induced by quasi-rectangle EPB shield tunneling. Journal of Zhejiang University (Engineering Science). 2018;52(2):317-24. (in Chinese).